remote sensing

MDPI

Article

Coastal Vulnerability Index Assessment Along the Coastline of Casablanca Using Remote Sensing and GIS Techniques

Anselme Muzirafuti [1,*] and Christos Theocharidis [2]

[1] Dipartimento Scienze Matematiche e Informatiche, Scienze Fisiche e Scienze della Terra, Università Degli Studi di Messina, Via F. Stagno d'Alcontres, 31-98166 Messina, Italy
[2] ERATOSTHENES Centre of Excellence, 3036 Limassol, Cyprus; christos.theocharidis@eratosthenes.org.cy
* Correspondence: anselme.muzirafuti@unime.it

Highlights

What are the main findings?

- DE Africa coastlines products revealed strong erosion along Casablanca's sandy shores, with a retreat up to −1.5 m/year.
- Coastal Vulnerabilty Index (CVI) results showed high vulnerability in low-elevation coastal zones where geomorphological landforms with low slope increase coastal exposure.

What is the implication of the main finding?

- The study demonstrates that freely available continental-scale products can effectively capture long-term shoreline behabiour and inform coastal risk evaluation in regions lacking in-situ monitoring.
- The proposed GIS-based workflow can serve as a replicable model for vulnerability assessment across other African coastal environments.

Abstract

This study explores the potential of Digital Earth Africa (DE Africa) coastlines products for assessing the Coastal Vulnerability Index (CVI) along the Casablanca coastline, Morocco. The analysis integrates remotely sensed shoreline data with elevation, slope, and geomorphological information from ASTER GDEM and geological maps within a GIS environment. Shoreline change metrics, including Shoreline Change Envelope (SCE), Net Shoreline Movement (NSM), Linear Regression Rate (LRR), and End Point Rate (EPR), were used to evaluate erosion trends from 2000 to 2023. Results show that sandy beach areas, particularly those below 12 m elevation, are highly exposed to erosion (up to 1.5 m/yr) and vulnerable to coastal hazards. Approximately 44% and 23% of the study area were classified as having very high and high vulnerability, respectively. The results indicate that remotely sensed data and GIS techniques are valuable and cost-effective tools for multi-scale geo-hazard coastal assessment studies. The study demonstrates that DE Africa products, combined with local landscape data, provide a valuable tool for coastal vulnerability assessment and monitoring in Africa.

Keywords: satellite-derived shoreline; coastal erosion; Digital Earth Africa; earth observation; coastal geomorphology; Landsat; coastal monitoring; climate change

check for updates

Academic Editors: Andy Steven and Javier Marcello

Received: 19 August 2025
Revised: 19 September 2025
Accepted: 3 October 2025
Published: 6 October 2025

Citation: Muzirafuti, A.; Theocharidis, C. Coastal Vulnerability Index Assessment Along the Coastline of Casablanca Using Remote Sensing and GIS Techniques. *Remote Sens.* **2025**, *17*, 3370. https://doi.org/10.3390/rs17193370

Copyright: © 2025 by the authors. Licensee MDPI, Basel, Switzerland. This article is an open access article distributed under the terms and conditions of the Creative Commons Attribution (CC BY) license (https://creativecommons.org/licenses/by/4.0/).

1. Introduction

In view of the current changes in the climate system and their impacts in coastal areas, the assessment of coastal vulnerability has become a topic of greatest interest [1–8]. For this reason, several methods have been proposed to determine coastal vulnerability, and they are mainly classified into four categories: indices, indicators, GIS, and dynamic computer models [1]. The most commonly used method to assess the coastal vulnerability is the CVI. This method was introduced by Gornitz [9] to evaluate coastal vulnerability by considering different physical factors that contribute to coastal erosion. Over the years, this method has been used by various authors [10–13], who have proposed improvements and novelties, which led to the creation of sub-methods that consider risk factors such as socio-economic factors for the Socio-Economic Vulnerability Index (SVI) and physical factors for the Physical Vulnerability Index (PVI) [1,13].

The physical risk factors, such as coastal slope, coastal elevation, coastal geomorphology, and shoreline dynamics, were adopted in the current study to assess the CVI of the Casablanca coastline. The coastline has been demonstrated to have important ecological functions and resource values for human survival and economic development [14–16]; thus, its monitoring and management are crucial. The Casablanca coastline was selected as a case study due to its high exposure to erosion, rapid urbanization, and increasing development pressures. Despite its significance, the region lacks long-term, spatially consistent products, offering harmonized multi-temporal shoreline data across Africa since 2000, and thus providing a unique opportunity to address this gap. Compared to local or regional datasets, DE Africa products ensure historical depth, spatial consistency, and scalability for both local and continental analyses. Previous CVI-related efforts in other regions have produced vulnerability maps based on different variables [17,18]. For example, Pantusa et al. [17], along the Calabrian Coastline, demonstrated that the shoreline erosion/accretion rates are among the most influential variables in CV studies. The studies conducted by Borzi et al. [19] and Foti et al. [20] analyzed the coastline evolution and environmental changes by studying shoreline dynamics, while Castelle et al. [21] and Konstantinou et al. [22] used satellite imagery to explore the potential of Earth observation (EO) data in the study of coastal area vulnerability. These studies highlighted the importance of using remote-sensing and GIS techniques for coastal area monitoring. These techniques are cost-effective and efficient for multi-temporal and multi-scale coastal vulnerability assessments. They can provide reliable and accurate results for long-term global shoreline change investigations [23–26].

Digital Earth Africa (DE Africa) [27] is the most ambitious program established in 2019 to leverage the power of remote-sensing EO technologies to produce products and provide services related to water resources and flood risk management, agriculture and food security, land degradation, coastline erosion, and services related to urbanization. This study aims to evaluate the potential of DE Africa Coastlines products [28] for CVI assessment on the coastline of Casablanca. While several studies analyzing coastal erosion, beach retreat, and shoreline retreat have been conducted on the Atlantic Coast of Morocco [29–32], this current study intends to analyze CVI on the coastline of Casablanca by using DE Africa Coastlines products in conjunction with local landscape information. According to the authors' knowledge, this study is the first of its kind conducted in this area by extracting and analyzing coastal erosion metrics such annual shoreline distances, SCE, NSM, LRR, and EPR with the main objective of evaluating CVI. The study focused on the coastline of Casablanca to evaluate how climate change has been affecting the sea level of the Atlantic Ocean and its effects on this coastal environment by identifying and analyzing its shoreline variabilities. The methodological approach used in this study could help decision makers mitigate and adapt to the effects of climate change in coastal areas. This study represents the first application of DE Africa Coastlines products for CVI assessment on the Casablanca

coastline. By integrating satellite-derived shoreline metrics with geomorphology, slope, and elevation data, we propose a transferable approach for vulnerability mapping in low-lying, rapidly urbanizing coasts. The use of annual shoreline rates from 2000 to 2023 adds a temporal dimension that is often lacking in conventional studies, allowing for the identification of long-term trends relevant for local planning.

2. Materials and Methods

2.1. Area of Study

Heger et al. [33] investigated coastal erosion, intending to evaluate recent trends and hotspots of coastal erosion in Algeria, Libya, Morocco, and Tunisia. The authors analyzed high-resolution EO data using 50 m resolution segments along the coastline and found that 54% of the Moroccan coastline is subject to erosion, with a long-term erosion of 0.9%. In general, the process of coastal erosion varies and depends on shoreline characteristics and the coastline's utilization. Casablanca, one of the Moroccan coastal cities, is the economic capital located northwest of the country on the Atlantic Ocean (Figure 1). Casablanca has districts like Anfa, Ain Sebba, and Sidi Bernoussi, the country's most important ports, and several industries. The study area is an ideal place to study the effect of climate change because it is at the junction of three environments, namely the ocean, land, and atmosphere, where we can observe the role played by every unit in the climate system. Due to its position and relationship with the Atlantic Ocean, Casablanca has winter precipitation influenced by several factors, such as the North Atlantic Oscillation and the atmospheric dampness of the west. The wind in areas with modifications in atmospheric pressure impacts the ocean in terms of currents and oceanic temperatures. In the current study area, the wind has S and SW directions in November till February and NNE and NW directions in April till September, with a 1.3 to 4.9 m/sec monthly average speed, but it can reach 43 m/s maximum value for instantaneous wind in winter at a frequency of 10.2 days/year [34].

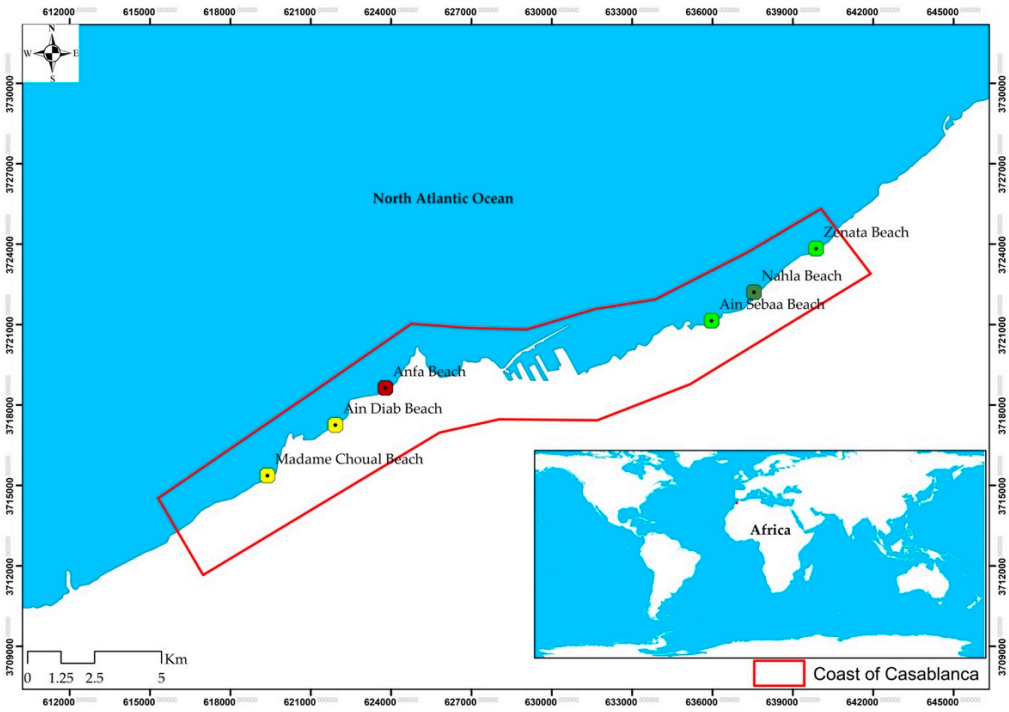

Figure 1. Map showing the location of the area of study on the coastline of Casablanca.

2.2. Methodology

2.2.1. Dataset and Software

In this study, DE Africa Coastlines products [35,36], geological maps, Advanced Spaceborne Thermal Emission, and Reflection Radiometer Global Digital Elevation Model version 2 (ASTER GDEM V2) with a spatial resolution of 30 m [37–39] were analyzed in a Geographic Information System (GIS) environment for the assessment of CVI. DE Africa Coastlines products contain information related to Africa's dynamic coastline from 2000 to 2023 for the whole African continent. These products have been generated following the same procedures as the Digital Earth Australia coastlines products [25]. The V0.4.2 version of DE Africa Coastlines products was accessed and downloaded from Amazon Web Services S3 [35]. They are grouped into two shapefile categories, polylines for the African annual shorelines that represent the median or 'most representative' position of the shoreline at approximately 0 m Above Mean Sea Level for each year since 2000 to 2023; and points for the African shoreline rate-of-change statistics, which are point datasets providing robust rates of coastal change for every 30 m along Africa's coastlines. The Centre de Suivi Ecologique, Dakar, has conducted a study to test the performance of the DE Africa Coastlines in collaboration with the member states of the WACA/ORLOA network (Investment Project for the Resilience of West African Coastal Zones/Regional Observatory of the West African Coast): Mauritania, Senegal, Gambia, Guinea Bissau, Republic of Guinea, Sierra Leone, Liberia, Côte d'Ivoire, Ghana, Togo, Benin, and Sao Tome, and Principe [35]. In each country, test sites were selected depending on the size of the portion of the coast, the availability of reference data, and the metadata associated with each type of data. The imagery for each country had a consistent accuracy of 5 m [35]. The analysis of the DE Africa Coastlines products (Table 1) allowed for a more detailed analysis of the coastline of Casablanca. Although the DE Africa Coastlines products are based on medium-resolution (30 m) Landsat imagery, the shoreline positions were validated to achieve a median horizontal positional accuracy of approximately 5 m. This level of accuracy, combined with its consistent multi-temporal coverage, makes the dataset appropriate for regional-scale shoreline change analysis in data-scarce environments such as Morocco's Atlantic Coast.

Table 1. Digital Earth Africa Coastlines products dataset descriptions [35,36].

Specification	Descriptions
Cell size—X (meters)	30
Cell size—Y (meters)	30
Coordinate reference system	ESPG:6933
Temporal resolution	Annual
Temporal range	2000–2023
Parent dataset	Landsat Collection 2 Surface Reflectance
Update frequency	Annual
Update latency	6 months from the end of the previous year
Product types	Annual coastlines: Rate of change statistics
Product names	coastlines_v0.4.2_shorelines_annual; coastlines_v0.4.2_rates_of_change
Data types	Shapefiles: polylines and points

2.2.2. Coastal Geomorphology—Lithology

The City of Casablanca, situated on the western limit of the Moroccan coastline, has two main rivers: Beth and Bourgreg. It also has big watersheds and several dams. In addition, the coastal region is drained by small rivers such as Oued Mellah, Oued Lakhdar, Oued Dir, Oued Merzeg, Oued Arrimena, and Oued Bouskoura. Each river has its watershed with variable shapes and different characteristics. The geological formations dominating

the coast of Casablanca are shale, sandstone, and quartzite; these formations constitute the folded Hercynian bedrock, which is affected by a network of faults dominating the NE-SW direction. The bedrock is visible in some coastal regions, but the rest is covered by secondary (Triassic and Cretaceous) formations and Tertiary formations dominated by limestone, and conglomerate; and Quaternary formations dominated by sand. The geomorphology of the Casablanca coast is characterized by sand beaches, rocky beaches, and artificial structures (Figure 2). In the ArcGIS software version 10.2.2, geomorphology–lithology information of the Casablanca coastline was obtained using visual interpretation and manual digitization approaches from geological maps and historical data [40].

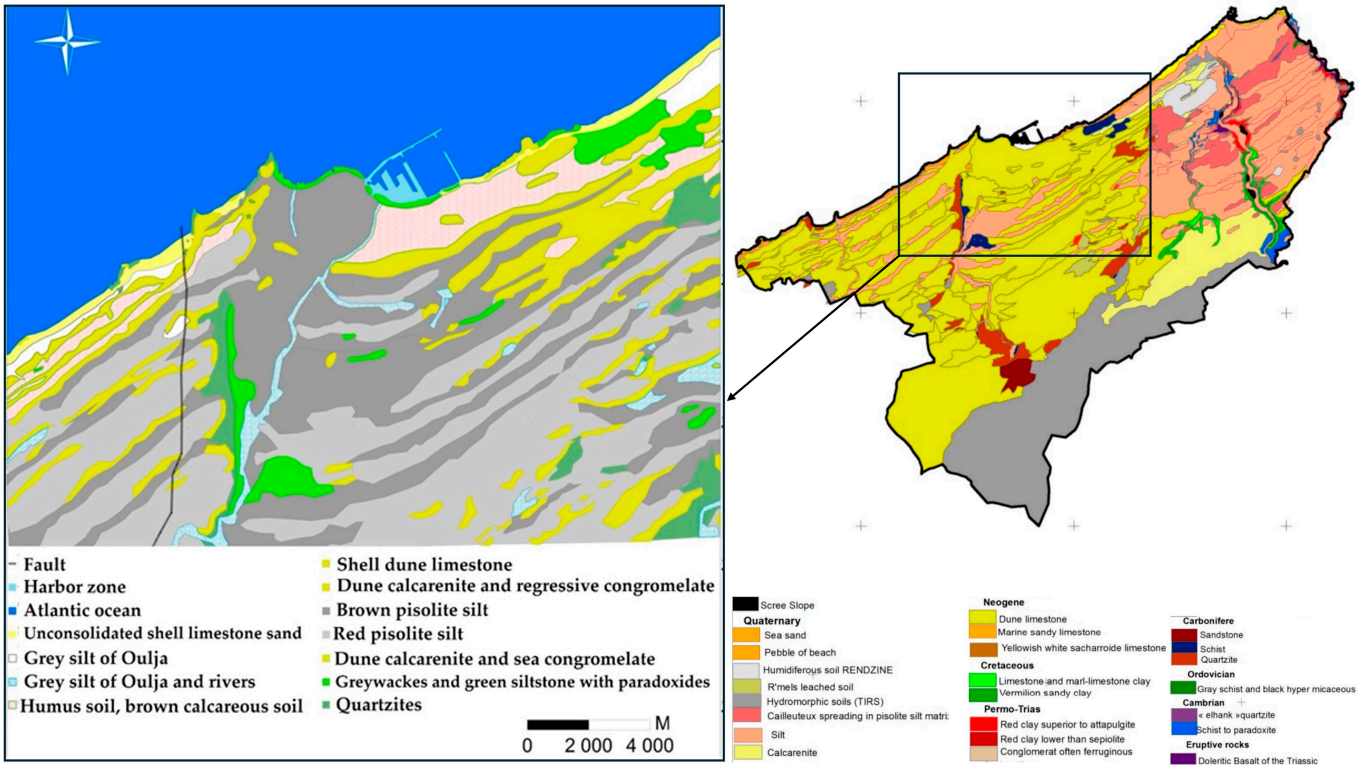

Figure 2. Extract of geologic map of Casablanca showing prominent geologic outcrops (modified from the geologic map of 1946 and Zerhouny et al. [40]).

2.2.3. Coastal Elevation

Coastal area elevation is an important factor in analyzing the behavior of the coastline concerning sea level rise. On the coast of Casablanca, information related to elevation was extracted from ASTER GDEM. The low-lying regions represent areas that are very vulnerable to rising sea levels. It is important to note that rising sea levels will amplify the erosion of beaches and accentuate land's submersion through the action of waves. Previous studies on the coastline of Casablanca–Mohammedia show evidence of ancient land movements and block falls generally located at the level of the coastal Corniche and other places. The geological context of Morocco and other countries of the Gulf of Cadiz (Spain, Portugal) is the source of tsunamis, which can destroy a large part of their coastlines (Figure 3), as noted by Omira et al. [41].

Regarding seismic risks, the Peak Ground Acceleration (PGA) maps calculated for a return period of 475 years show values between 0.04 g and 0.08 g, indicating that the Casablanca site would have an intensity in the order of V corresponding to a moderate level of damage. This allowed us to envisage an intensity in the order of lower than V for 50 years. However, such intensity estimates for PGA values do not consider local geolog-

ical or topographical conditions that can amplify seismic movements [42]. Concerning tsunami risks, historical events and seismotectonic contexts indicate that the Moroccan west coast is exposed to relatively significant tsunami risks with wave heights of 2 m and 1 m compared to the events of 1 November 1755 and 28 February 1969. In the next 20 years, there is estimated to be about a 10% probability of a wave of 1 m in height on the coastline of Casablanca [42]. Analysis of altimetry data shows that from 15 January 1993 to 15 December 2014, the sea level at the coast of Casablanca increased by 2.6 mm/year. This rise in sea level is partially due to the global melting of glaciers and ice sheets, continental water exchange with the ocean and the Gibraltar Strait, rising ocean temperature, and glacial isostatic adjustment. It is also important to note that the 30 m spatial resolution of the ASTER GDEM may affect the accuracy of the derived elevation maps and slope values, particularly in narrow, steep, or highly variable coastal areas. This issue reflects the well-documented scale dependency in geospatial analyses, similar to the British coastline paradox [43], where the measured length of coastlines varies depending on the measurement resolution. Although finer-resolution elevation models (e.g., ALOS-DEM, EU-DEM, and UAV-derived DEMs) would offer more detail, ASTER GDEM was used to ensure consistency with the 30 m resolution of the DE Africa Coastlines datasets.

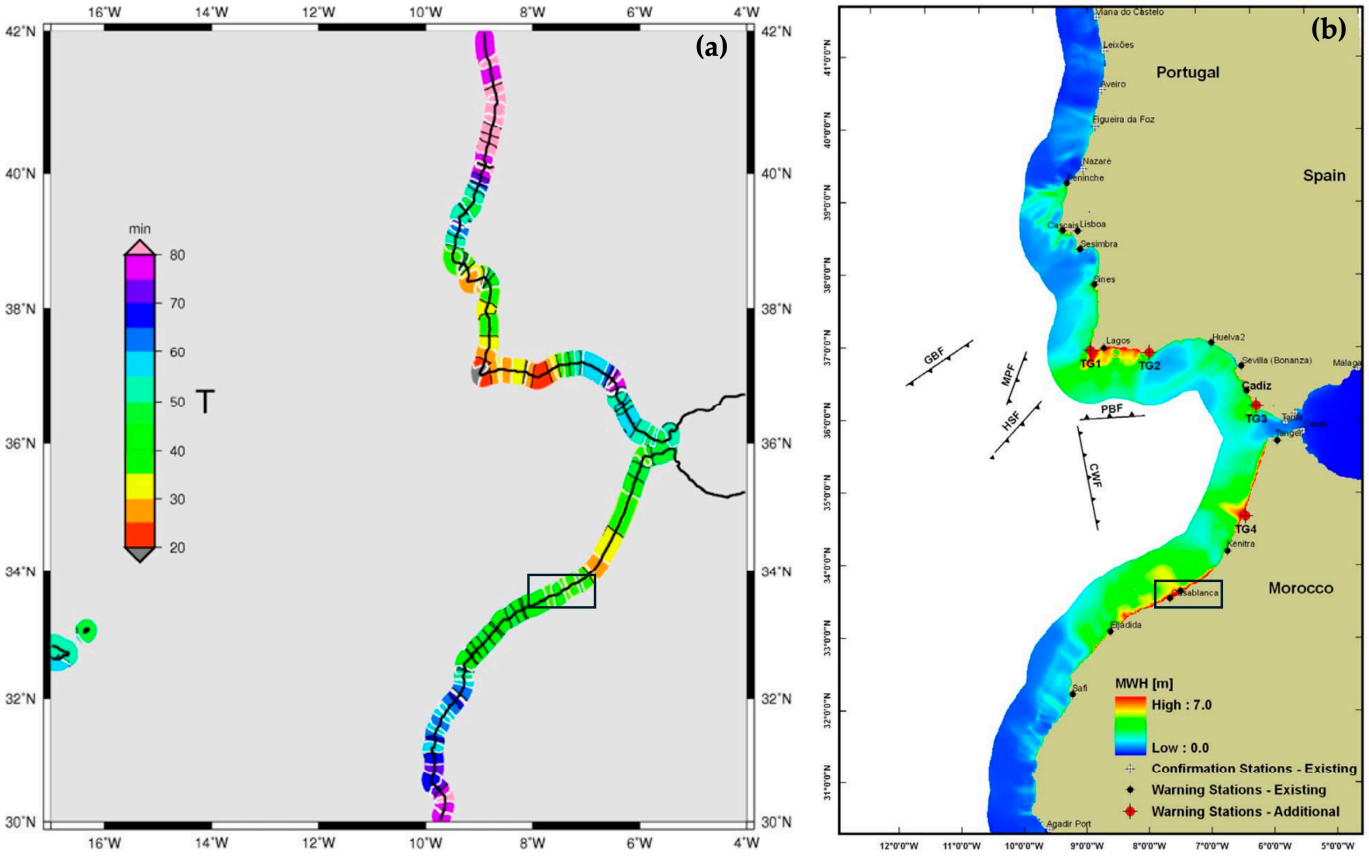

Figure 3. Digital maps showing (**a**) the minimum travel time to arrive at the shore estimated for five sources (GB, MPF, HSF, PBF, and CWF); and (**b**) the maximum wave height for the 5 Tsunami sources of the coastline of Casablanca, modified from Omira et al. [41].

2.2.4. Coastal Slope

The slope is an important parameter in the study of the impact of sea level rise, as it not only makes it possible to estimate the relative risks of flooding of the shore but also influences the velocity of change in the coastline for shrinkage regions with low slope values. Ten percent of the Casablanca coastline has a slope ranging from 0 to 4%, with areas

likely to be affected by the rise in sea level, which is accompanied by surges, storms, and the action of waves. The slope was calculated from a Digital Elevation Model (ASTER DEM), using the Horn 1981 [44] method, available in the ArcGIS spatial analyst and useful for beach morphology change studies [45].

2.2.5. Shoreline Dynamics

The coastline of Casablanca is subjected to a range of pressures, including extreme weather and climate, sea level rise, and human development. Understanding how this coastline responds to these pressures is important for managing this region from social, environmental, and economic perspectives. The DE Africa Coastlines products are continental datasets that include annual shorelines and coastal change rates along the entire African coastline from 2000 to 2023. These products combine satellite data from the DE Africa program with tidal modeling to map each year's typical coastline location at mean sea level. Based on a tidal mode, the mapped shoreline corresponds to the median waterline position at approximately 0 m above mean sea level. The products enable coastal erosion and growth trends to be examined annually at both a local and continental scale, and for patterns of coastal change to be mapped historically and updated regularly as data continue to be acquired. The ability to map shoreline positions for each year provides valuable insights into whether changes to the coastline resulting from particular events or actions, or a process of more gradual change over time [35,36]. Such analyses were conducted in this study. A database of annual shorelines (Figure 4) and 1630 points of those products was created and analyzed in ArcGIS.

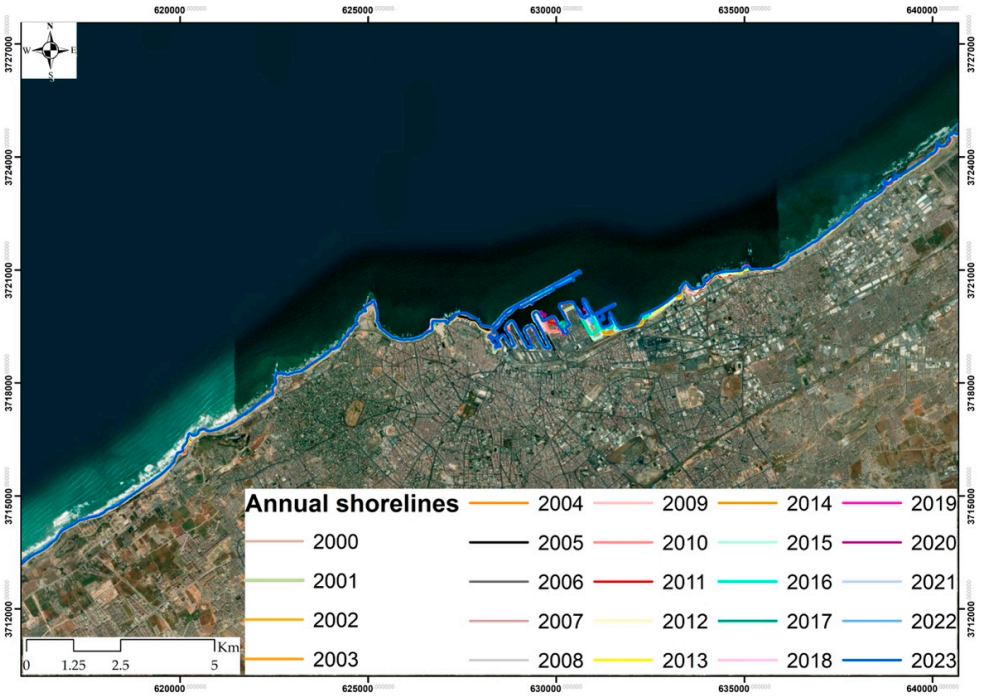

Figure 4. Annual shorelines on the coast of Casablanca obtained from DE Africa Coastlines v0.4.2.

Locations of measured points containing rate-of-change statistics for every 30 m along the coast of Casablanca were obtained from DE Africa Coastlines v0.4.2 and were used to calculate coastal erosion metrics such as End Point Rate (EPR), which indicates the rate of change between the oldest and the youngest shoreline for each transect; and Linear Regression Rate (LRR), which is a regression statistic estimated by fitting a least-squared regression line to all shoreline points of a transect. LRR represents the change in m/yr occurring on each transect. It is determined by plotting the shoreline intersect positions

(distance from baseline) with respect to shoreline date (time); in this case, all the data (annual shoreline positions) are used, regardless of changes in trend or accuracy, as presented in Figure 5. In this study, the EPR and LRR were used in conjunction with variables to calculate the CVI. The EPR is calculated by dividing the displacement distance by the time that has elapsed between the oldest and the most recent shoreline. The results indicated the accretion (for positive values) and the erosion (for negative values) for the study area.

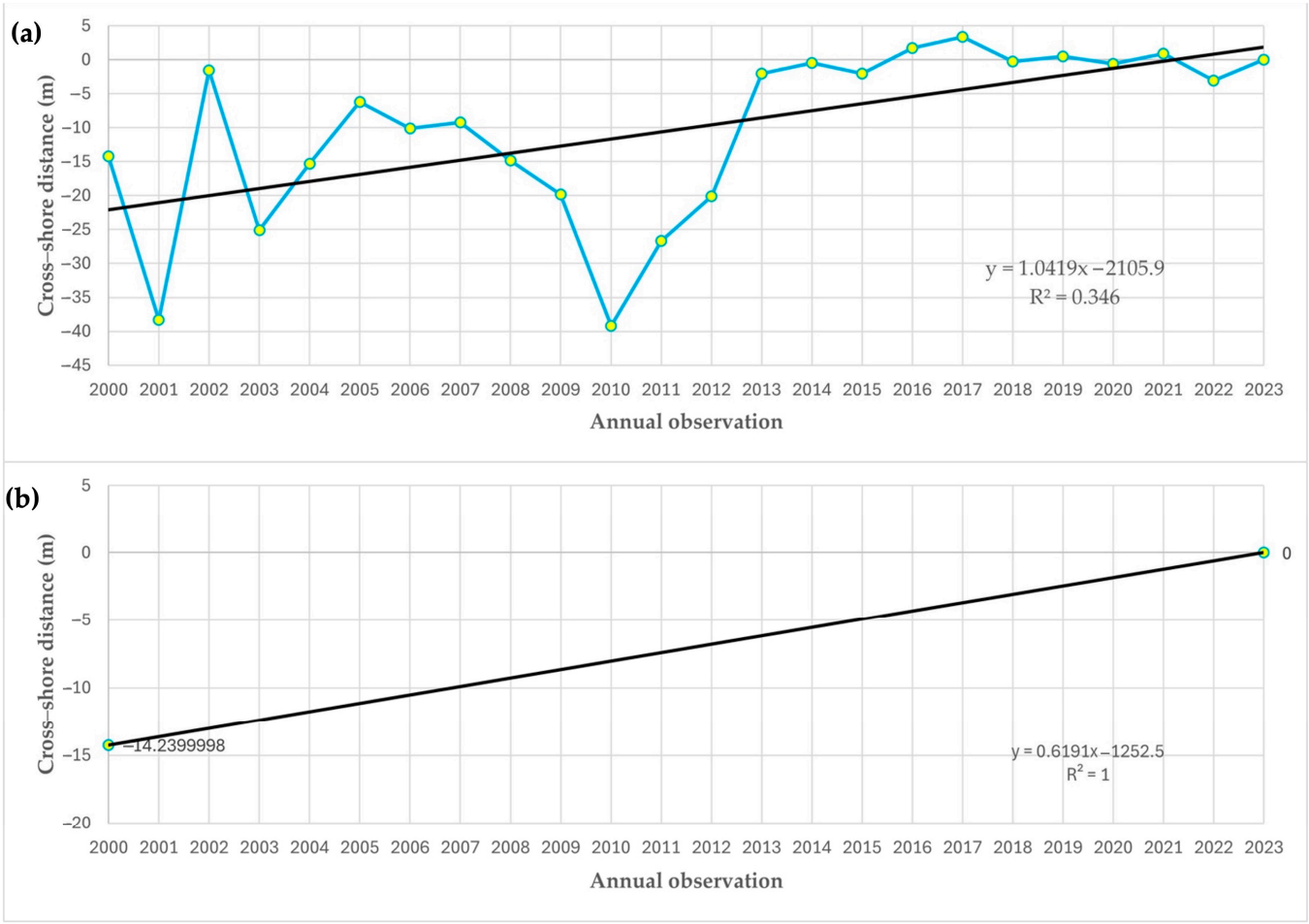

Figure 5. Illustrations of LRR and EPR calculations using annual shoreline distances. This illustration is an example of the measured point 0 located on the coast of Casablanca, Morocco (the beach at the Zenata segment). (**a**) LRR is calculated by considering all cross-shore annual shoreline positions where the slope of the equation equals the rate of change (1.0419 m/yr). (**b**) EPR is calculated by considering cross-shore positions of the oldest annual shoreline (2000) and most recent annual shoreline (2023) where the slope of the equation equals the rate of change (0.6191 m/yr). Detailed descriptions of this point considered for LLR and EPR calculations are presented in Supplementary Materials S.1 (Table S1).

DE Africa Coastlines products also allowed us to compute (Equations (1)–(3)) distance measurements in meters, such as NSM, which indicates the distance between the oldest and the recent shoreline for each point; and the Shoreline Change Envelope (SCE), which indicates a measure of the maximum distance of change or variability among all annual shorelines (Figure 6). SCE is calculated by computing the distance between two annual shorelines intersecting a given transect.

$$Y = (ax + b) \quad (1)$$

$$NSM = (do - di) \quad (2)$$

$$\mathrm{EPR} = \frac{(do - di)}{(to - ti)} \tag{3}$$

where *di* is the distance of the oldest shoreline, *do* is the distance of the recent shoreline, *ti* is the shoreline date (time) of the oldest shoreline, *to* is the shoreline date (time) of the recent shoreline, a is the slope of the equation describing the LRR of the linear regression equation of Y, and *b* is a constant.

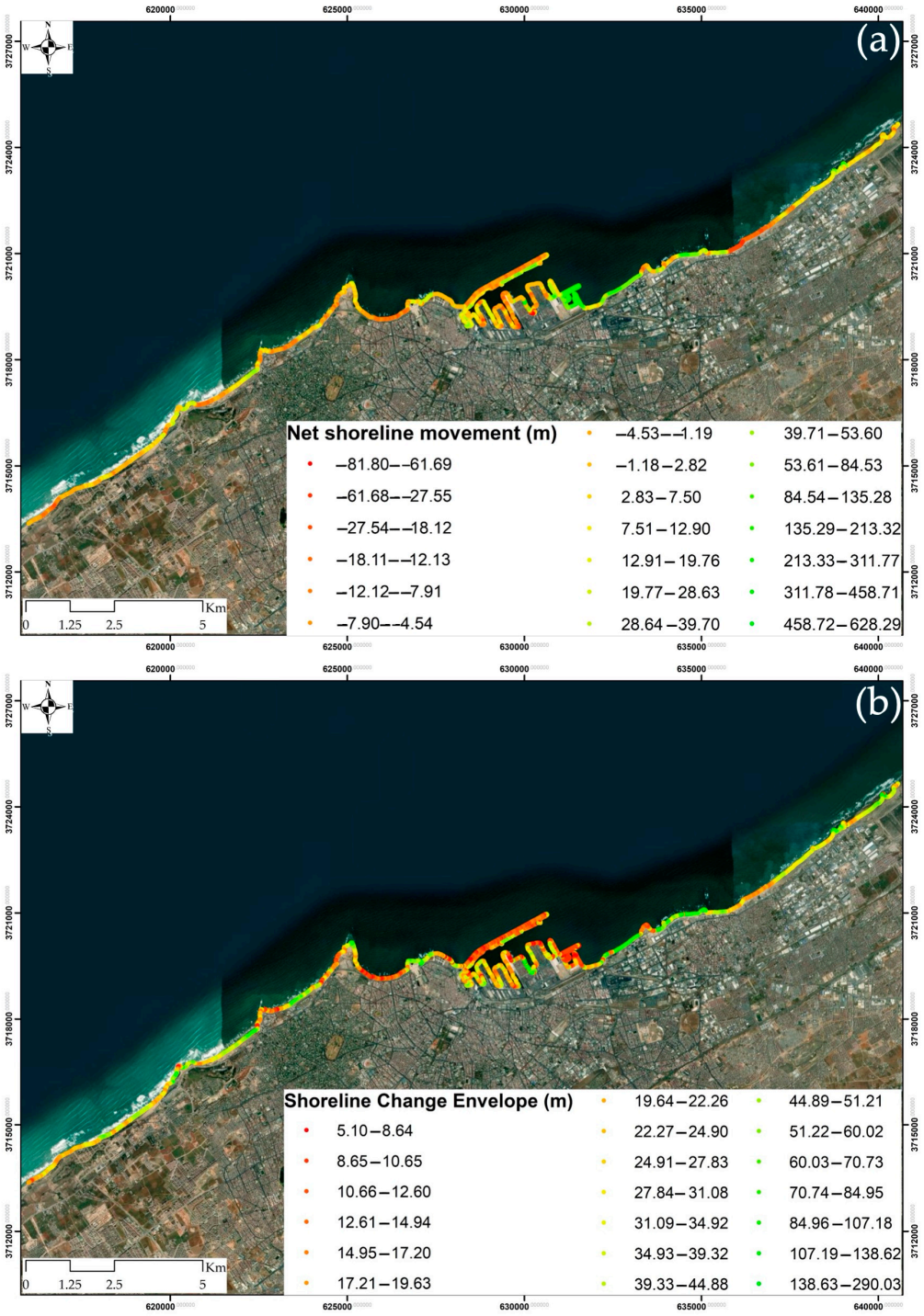

Figure 6. (**a**) NSM on the coast of Casablanca. It is the distance between the oldest shoreline (2000) and the most recent annual shoreline (2023). Negative values indicate that the coastline retreated between 2000 and 2023, while positive values indicate the growth of the coastline. (**b**) Map depicting the Shoreline Change Envelope (SCE) on the coast of Casablanca. Information related to the location of 1630 points is presented in Supplementary Materials S.2 (Figure S1).

The combination of EPR, LRR, NSM, and SCE was selected to capture both the temporal trends and spatial variability of shoreline change. EPR and LRR provide insights into long-term trends in erosion and accretion, which are essential for understanding the rate and direction of coastal change. In contrast, NSM quantifies the net positional change between endpoints, while SCE reflects the maximum observed variability across all annual shoreline positions. Together, these metrics offer a robust representation of shoreline dynamics, enabling a more comprehensive and practical coastal vulnerability assessment.

2.2.6. Coastal Vulnerability Index Calculation

Information obtained from different coastal variables, such as coastal geomorphology–lithology, coastal slope, shoreline dynamics (erosion/accretion), and coastal elevation, were used to compute the CVI using Equation (4), which integrates all of these variables (Table 2). While it is well known that there is no universally fixed equation for calculating CVI, methodological approaches are typically adapted to the specific morphological characteristics of the study area, such as surface features, geological settings, and local coastal processes. The four variables in this study were selected based on their physical relevance to coastal vulnerability and their frequent application in previous CVI frameworks. These parameters have consistently been identified in the literature as key indicators of coastal risk, especially in areas experiencing rapid shoreline changes and low-lying topography. Additionally, these variables were chosen based on data availability, quality, and their capacity to capture the dominant processes influencing vulnerability along the Casablanca coastline. In this study, the CVI was calculated as the geometric mean of the ranked variables. The use of the geometric mean rather than the arithmetic mean was chosen because it reduces the influence of extreme values and provides a balanced representation of the combined effect of multiple factors, which is particularly appropriate in multi-criteria assessments such as CVI. Equal weighting of the four variables was applied following a common practice in previous CVI applications, where, in the absence of a universally accepted weighting scheme, equal weighting ensures that no single factor disproportionately drives the index.

$$CVI = \sqrt{(V1 * V2 * V3 * V4)}/4 \quad (4)$$

Table 2. Variables used to calculate the Coastal Vulnerability Index.

ID	Variable	Ranking of Coastal Vulnerability Index			
		Low 1	**Moderate 2**	**High 3**	**Very High 4**
V1	Coastal geomorphology	Rocky areas: quartzites, greywackes, and shales		Calcarenite dunes; protected sandy beaches	Sandy beaches
V2	Coastal slope (%)	>12	8–12	4–8	0–4
V3	Altitude (m)	>9	6–9	3–6	0–3
V4	Shoreline dynamics (m/yr)	>+1–>0	<0–≥−1	<−1–≥−2	<−2

3. Results

In this study, the CVI was calculated to assess the vulnerability of the Moroccan Atlantic Coast in Casablanca. The CVI was analyzed using remote-sensing and GIS techniques, namely the DE Africa Coastlines products and ASTER GDEM, as well as a geological map in a GIS environment. The CVI was calculated based on four variables (coastal elevation, coastal slope, coastal geomorphology–lithology, and shoreline dynamics). Figure 7 depicts the vulnerability of the coast of Casablanca based on its geomorphology. Very high vulnerability was observed in areas occupied by sandy beaches in the NE and SW of Casablanca,

while high and moderate vulnerability were observed on natural and semi-natural coasts occupied by hard rocks.

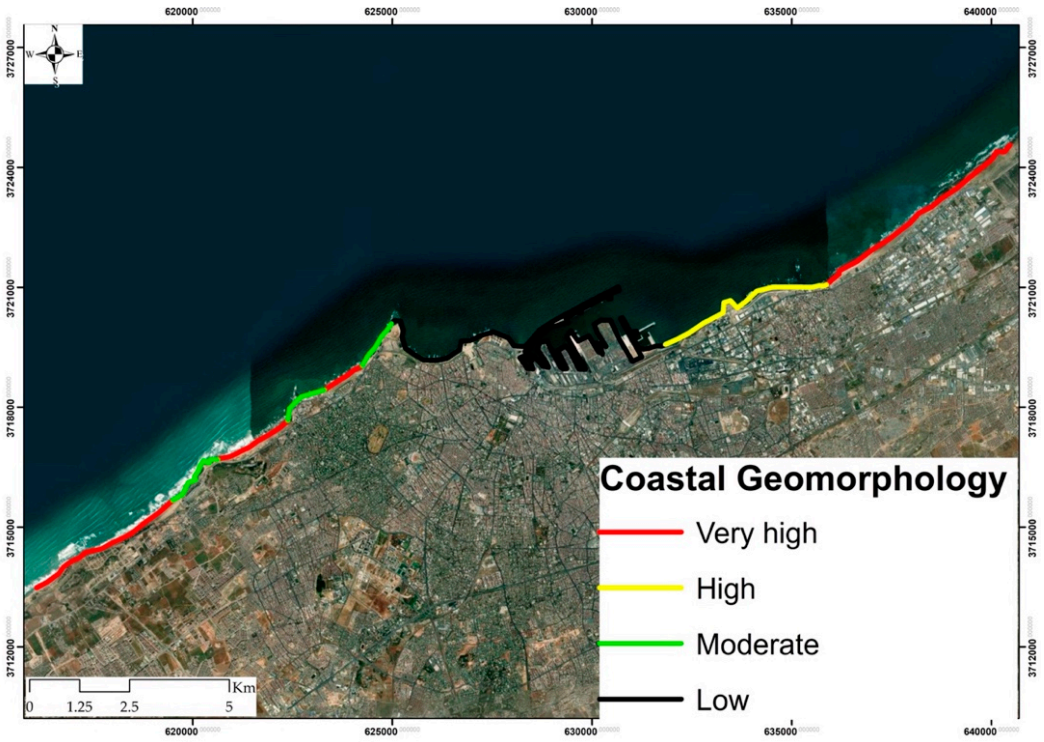

Figure 7. Coastal geomorphology variable ranking was used to calculate the CVI calculation.

Figure 8 illustrates the vulnerability ranking of the coast of Casablanca concerning the coastal slope (steepness from each coastal cell of an elevation raster with 30 m of spatial resolution) and coastal elevation (vertical distance of a point above the mean sea level). Very high vulnerability was observed on sandy beaches, while high and moderate vulnerability were observed on natural and semi-natural coasts occupied by hard rocks.

For each point, the rates of change were calculated by linearly regressing the annual shoreline cross-shore position against the annual observation, as presented in Figure 5. Negative values indicate the retreat, while positive values indicate the growth of the coastline. However, the annual shorelines do not reflect shorter-term coastal variability, such as changes in shoreline position between low and high tide, seasonal effects, or short-lived influences of individual storms. In this case, annual shorelines could show lower variability than the true range of coastal variability observed, and the rates of change do not assign a reason for change, nor do they necessarily represent processes of coastal erosion or sea level rise [35,36]. For these reasons, the rates of change (Figure 9) should be interpreted with caution. Therefore, six sand beaches were chosen to better analyze the shoreline dynamics related to coastal erosion and accretion. In this regard, the coastline of Casablanca, from 2000 to 2023, had a high rate of erosion, of about −1.45 m/yr and −1 m/yr, calculated on the Beach of Ain Sebaa for EPR and LRR, respectively. This phenomenon affected the regions occupied by the sand beaches, which had low protection against the tides and human activities. Almost the entire coastline of Casablanca is affected by erosion, with a high rate observed in the regions occupied by Quaternary formations and a low rate in the areas occupied by hard rocks and man-made structures. In the northeast of Casablanca, on the Beaches of Zenata, Anfa, and Ain Diab, the shoreline variation is continuous, with erosion persisting in these areas. On the Port and Marina of Casablanca and its western part, the position of the shoreline is irregular in times with alternation of erosion and

accretion processes. In general, the CVI (Figure 10) calculated indicates that the coastline of Casablanca is vulnerable, and some parts of its coastline need changes in practice and protection against the effects of extreme weather and human activities, particularly the eastern part at Zenata, where the city reaches the highly vulnerable coastline.

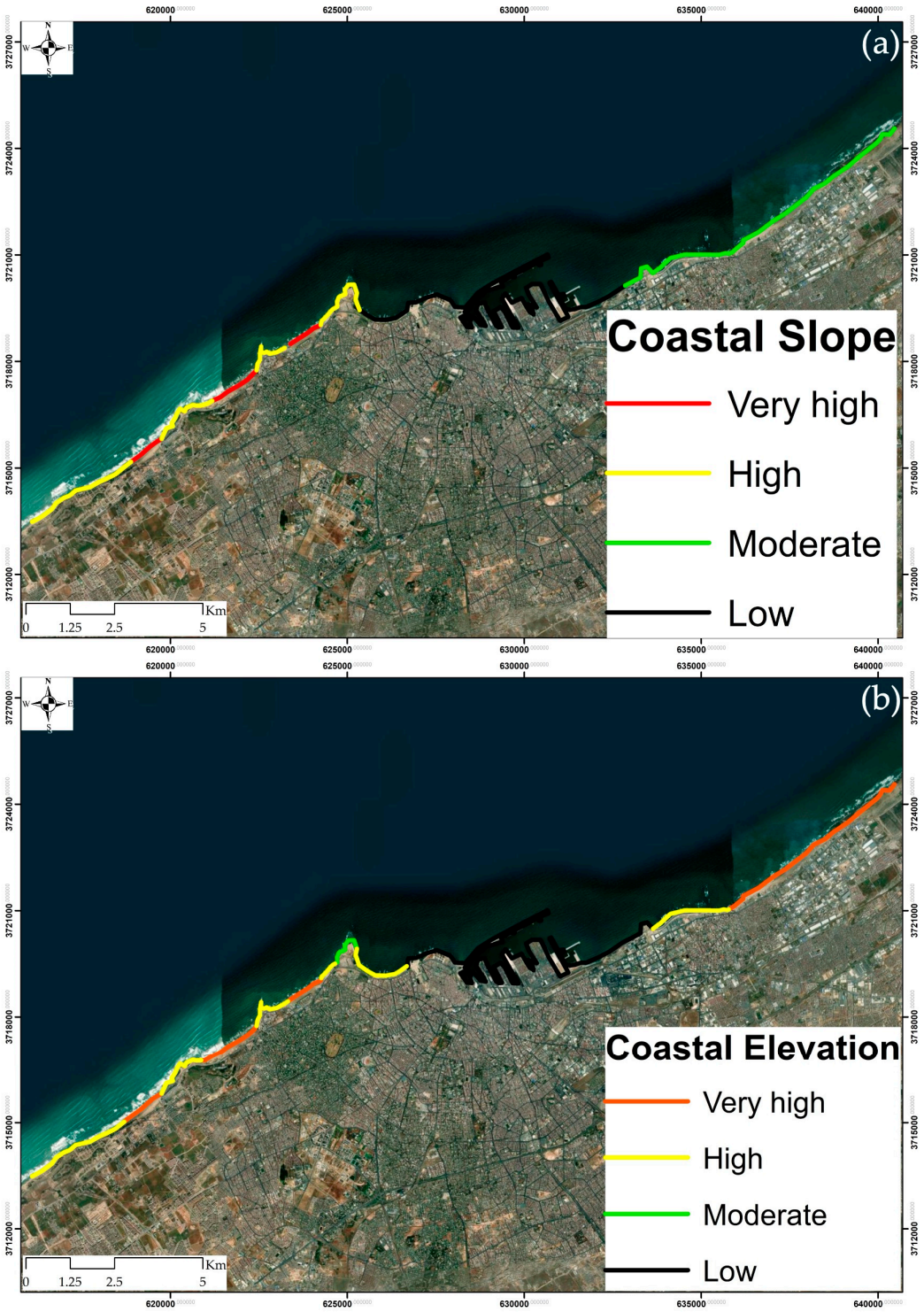

Figure 8. Rankings of variables used to calculate the Coastal Vulnerability Index: (**a**) coastal slope and (**b**) coastal elevation.

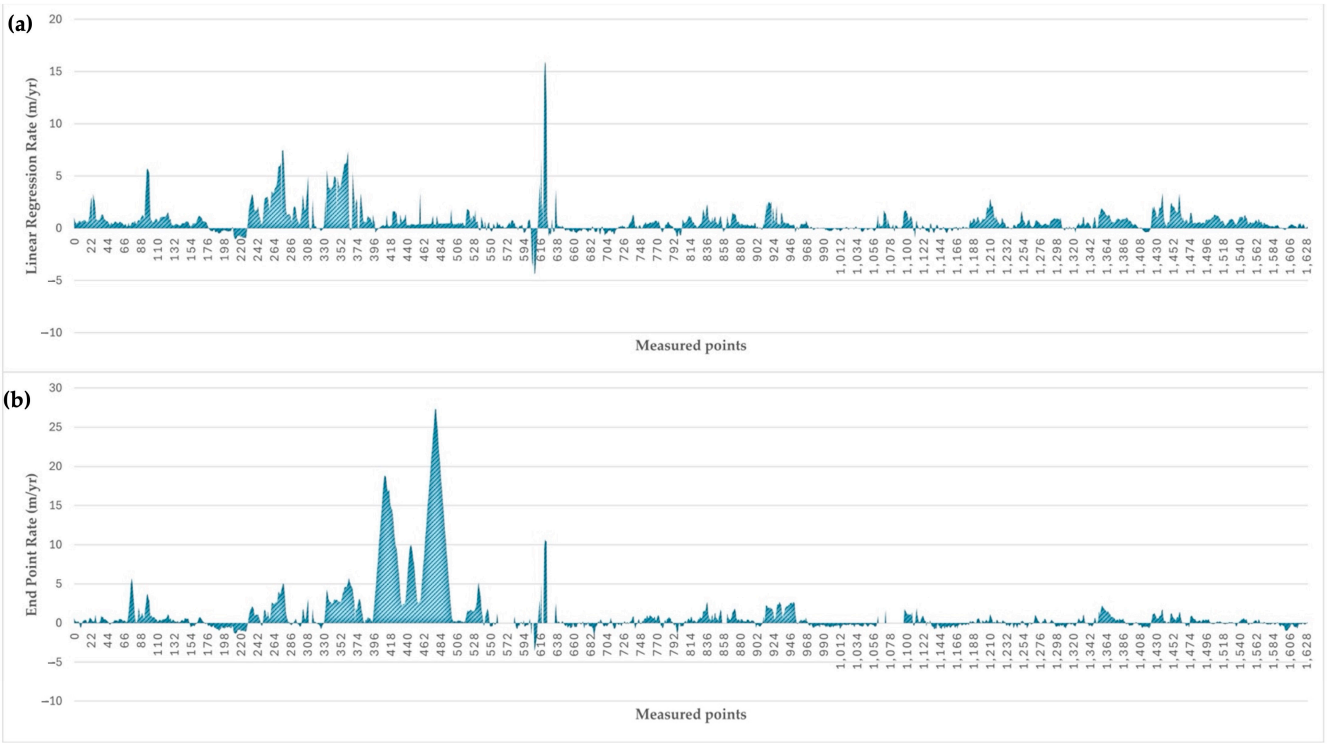

Figure 9. Annual rates of change for 1630 points located on the coast of Casablanca. LRR revealed the coastline growth reaching 16 m/yr and the retreat of about −4 m/yr near the port of Casablanca (**a**), while EPR indicated the coastline growth of about 28 m/yr and a retreat of about −3 m/yr (**b**). Information related to the significance (*p*-value) and the standard error of the linear relationship between the annual shoreline cross-shore positions and the annual observations is presented in Supplementary Materials S.3 and S.4 (Figures S2 and S3).

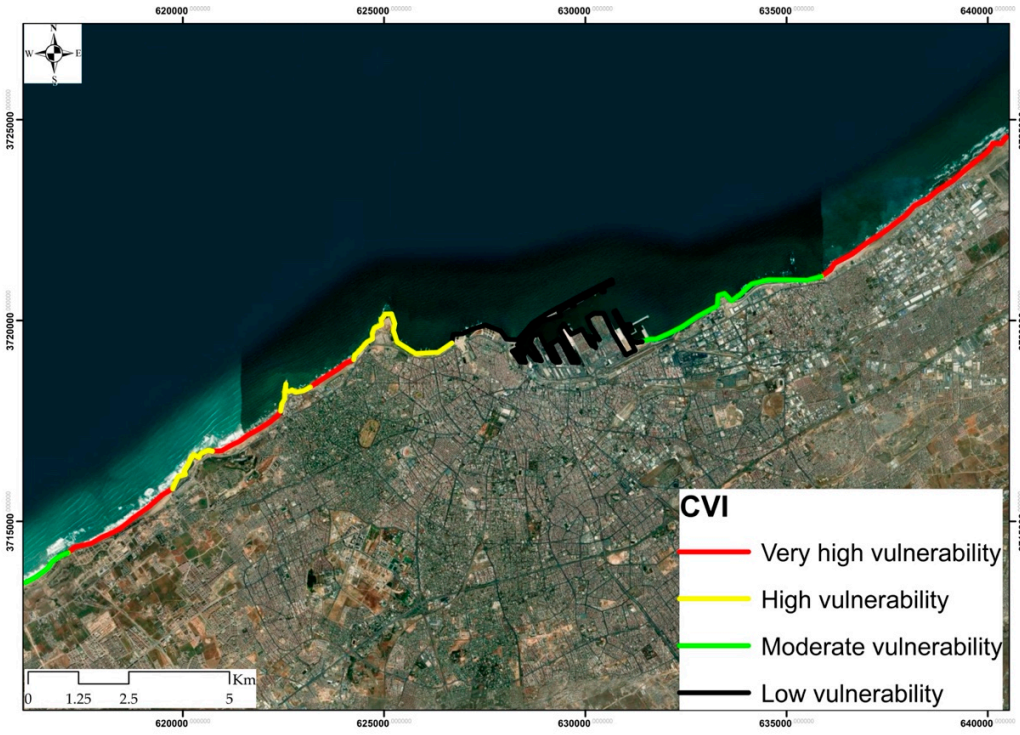

Figure 10. The CVI of the coast of Casablanca indicates very high vulnerability on sand beaches. High vulnerability was observed on semi-rocky areas, moderate vulnerability was observed on semi-rocky areas, and low vulnerability was observed on artificial areas.

Figure 11 depicts the proportion of the CVI, indicating that 43.95% and 23.03% of the Casablanca coastline have, respectively, a very high and high vulnerability index, and they are vulnerable to natural phenomena such as inundation, coastal flooding, and submersion, while 7.58% and 25.44% have, respectively, moderate and low vulnerability. The northeast and southwest of the coastline of Casablanca are more vulnerable due to a lack of protection for areas occupied by sandy beaches, while the areas occupied by hard rocks or cliffs are less vulnerable. However, in the central part of the harbor of Casablanca, the artificial coastline is occupied by constructions and is well protected.

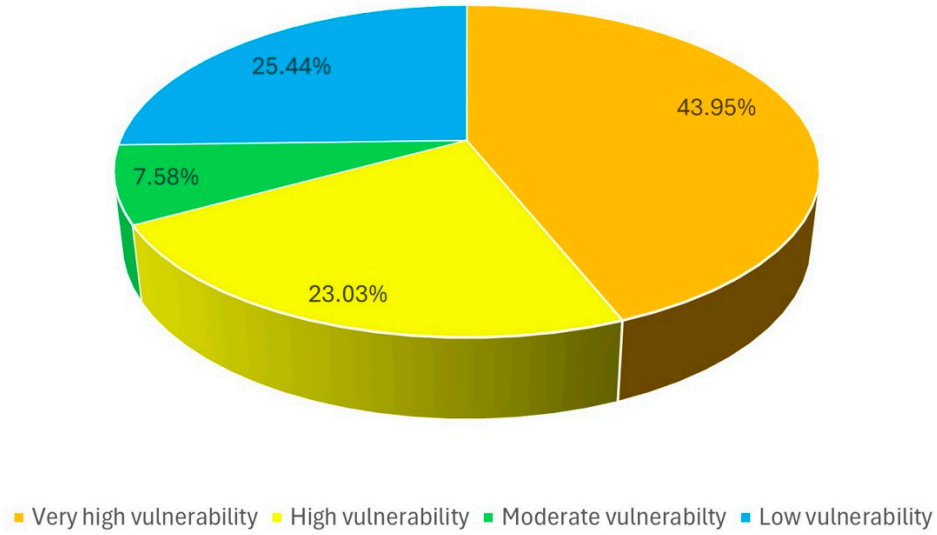

Figure 11. Repartition of the Coastal Vulnerability Index for the coast of Casablanca.

4. Discussion

4.1. Annual Rates of Change and Coastline Classification for the Beaches of Madame Choual, Ain Diab, Anfa, Ain Sebaa, Nahla, and Zenata, Located on the Coastline of Casablanca

The study conducted by Pantusa et al. [17] showed that the shoreline rates of change are among the most influential variables in the assessment of the coastal vulnerability (CV); to further evaluate the contributions of the LRR and the EPR to the vulnerability of the coastline of Casablanca, very detailed shoreline dynamics were performed on six beaches, namely Madame Choual (Figure A1; Table A1), Ain Diab (Figure A2; Table A2), Anfa (Figure A3; Table A3), Ain Sebaa (Figure A4; Table A4), Nahla (Figure A5; Table A5), and Zenata (Figure A6; Table A6). The ability to calculate the rate of change in the shoreline for each 30 m along the coastline of Casablanca provides a huge opportunity to identify the areas affected by erosion and accretion. This information is beneficial for determining how such geological processes contribute to coastal vulnerability. The level of detail offered by this point-based analysis for six distinct beaches is rarely explored in CVI studies, particularly in Africa. By applying both LRR and EPR at 30 m intervals along the shoreline, this study provides spatially explicit insights into how vulnerability differs across small-scale geomorphic units. Notably, discrepancies between LRR and EPR values were observed at several locations, particularly between measured points 396 and 484 (Figure 9). In this segment, EPR shows a pronounced peak of up to 28 m/yr, while LRR remains substantially lower. This difference reflects a non-linear shoreline behavior, where significant accretion occurred near the end of the time series. Since EPR only considers the net change between the oldest and most recent shoreline, it captures such abrupt, recent changes more strongly. In contrast, LRR averages all shoreline positions over time, thus dampening short-term variation. This highlights the value of using both metrics to capture different dimensions of shoreline dynamics.

The sandy Beach of Madame Choual is located on the southwest (SW) of Casablanca, near the commercial centre of Morocco Mall. Analysis of the 49 points obtained from the DE Africa Coastlines products, as presented in Figure A1, revealed accretion of the coastline of about 77.5% and 75.5% (Table A1), concerning the results obtained by LRR and EPR. Also, a low vulnerability index was observed, probably due to the morphology of the beach protected by natural and semi-natural features located in the NE, contrary to the SW, where moderate erosion was observed. The rates of change calculated for 71 points along the coast of the Beach of Ain Diab (Figure A2) indicated moderate erosion of about 18% and 42% (Table A2) for both LRR and EPR, respectively. The assessment of the CV indicated that its index varies from moderate to low vulnerability, mainly due to its configuration. Meanwhile, Figure A3 showed that the rates of change calculated for 44 points located on the Beach of Anfa varied from 93.18% to 6.82% for LRR and from 59.1% to 38.63% for EPR, with low vulnerability observed for a large part of the beach (Table A3).

In addition, on the Beach of Ain Sebaa, the rates of change calculated for the 43 points (Figure A4) highlighted areas affected by moderate to low vulnerability (Table A4). Furthermore, the rates of change calculated for 95 points located on the Beach of Nahla (Figure A5) illustrated a trend of shoreline changes dominated by erosion of about −1.4 m/yr, as obtained with EPR, and moderate accretion of about 1.5 m/yr for LRR, with both indices revealing high-, moderate-, and low-vulnerability areas (Table A5). Analyses conducted for 76 points on the Beach of Zenata (Figure A6) pinpointed the importance of evaluating the shoreline dynamics with two more indices for CVI assessment. LRR indicated that from 2000 to 2023, the Beach of Zenata experienced accretion with low vulnerability, while EPR was able to provide information related to erosion with a rate of about −1 m/yr (Table A6).

In general, the rates of change calculated for these six beaches revealed low CVI with moderate accretion at the rates of 82% and 63%, moderate CVI with moderate erosion at the rates of 17% and 34%, and high CVI with high erosion at the rates of 0.89 and 3.06 for LRR and EPR, respectively; no very high CVI was observed for LRR or EPR (Figure 12).

Nevertheless, due to the limited availability of consistent datasets for Casablanca, the validation of DE Africa-derived shoreline change rates against in situ data such as local tide gauges, long-term beach profile surveys, or official erosion reports was not conducted. However, as mentioned earlier, the coastlines of the DE Africa Coastlines have undergone continental scale calibration/validation process with median horizontal positional accuracy of ~5 m, supporting their reliability for regional assessments. In our case, in situ field observations from 2015 were used to confirm shoreline positions and coastal features qualitatively, and these were consistent with the spatial patterns of high and very high vulnerability identified. Additionally, Chtioui et al. [46] analyzed the storm's influence on shoreline evolution along Casablanca–Mohammedia coastline, using historical aerial photographs, wave analysis data, Landsat data, GIS tools, and statistical methods. The authors evaluated spatial and temporal changes in the shoreline from 1969 to 2020. Their findings indicated that approximately 39% and 61% of the studied area have experienced erosion and accretion, respectively, with no clear correlation with storm parameters. However, it is important to note that the analyses were conducted for five shorelines of 1962, 1982, 1997, 2009, and 2020, which would not allow for an accurate evaluation of the temporal influence of the storm events on shoreline movement. On the one hand, the DE Africa's annual shoreline positions (Supplementary Materials) are consistent with the yearly distribution of the wave parameters (Figure 13), with a higher wave height leading to the movement of the shoreline toward the land, especially in 2008, 2011, and 2014. On the other hand, DE Africa Coastlines products' rates of change for the Casablanca coastline coincide with yearly storm energies, as the lowest cumulative energy leads to shoreline erosion at a significant rate, while the highest cumulative energy

leads to accretion with a high rate of change. Flooding episodes along the coastline of Casablanca–Mohammedia [47] frequently occur at high tide, with the most vulnerable zone identified on sandy beaches, and such coastal hazards are projected to grow.

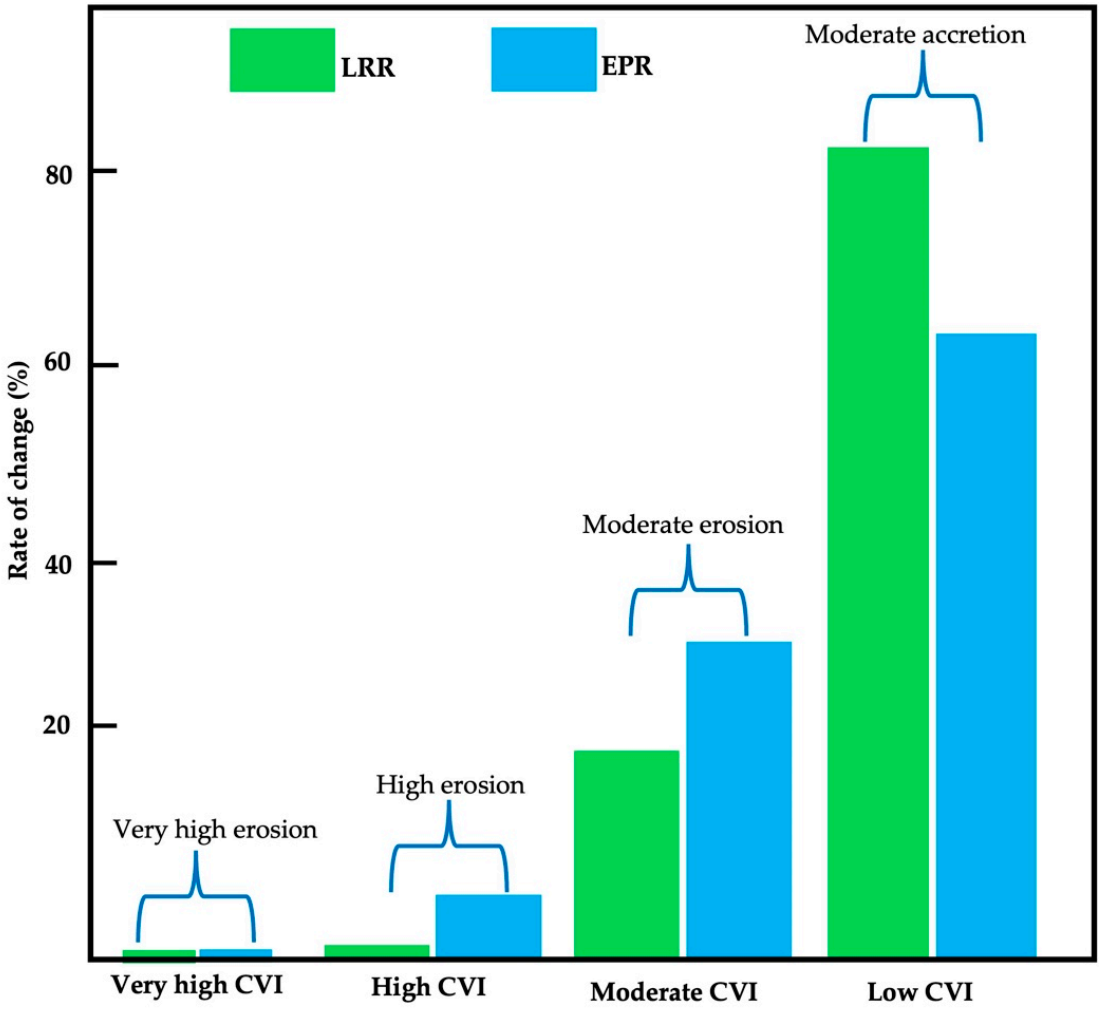

Figure 12. Distribution of shoreline change categories by CVI class for the six beaches on the Casablanca coast, based on LRR and EPR. The bars represent the percentage of shoreline segments under each CVI class experiencing very high, high, and moderate erosion, and moderate accretion. The figure illustrates how erosion intensity corresponds to CVI levels, with higher vulnerability classes generally linked to higher erosion rates, and lower vulnerability classes associated with moderate accretion. Differences between LRR and EPR highlight the impact of temporal variability in shoreline change detection.

4.2. Implications for Coastal Areas Management

This study reveals that DE Africa Coastlines products can be used for coastline dynamics studies and the assessment of coastal vulnerability of the whole African continent. Such studies could provide helpful information about particular events or processes affecting African coastal regions. In the context of climate change, monitoring the shoreline and managing coastal areas are becoming increasingly important because they directly affect the coastal environment and economic development. By analyzing the LRR and EPR [48], future shoreline position can be predicted [49–53] and help prepare for future changes which could affect the coasts and effectively mitigate the impacts of hydrogeological events aggravated by climate change, such as sea level rise, severe storms, coastal submersion, and saltwater intrusion [54].

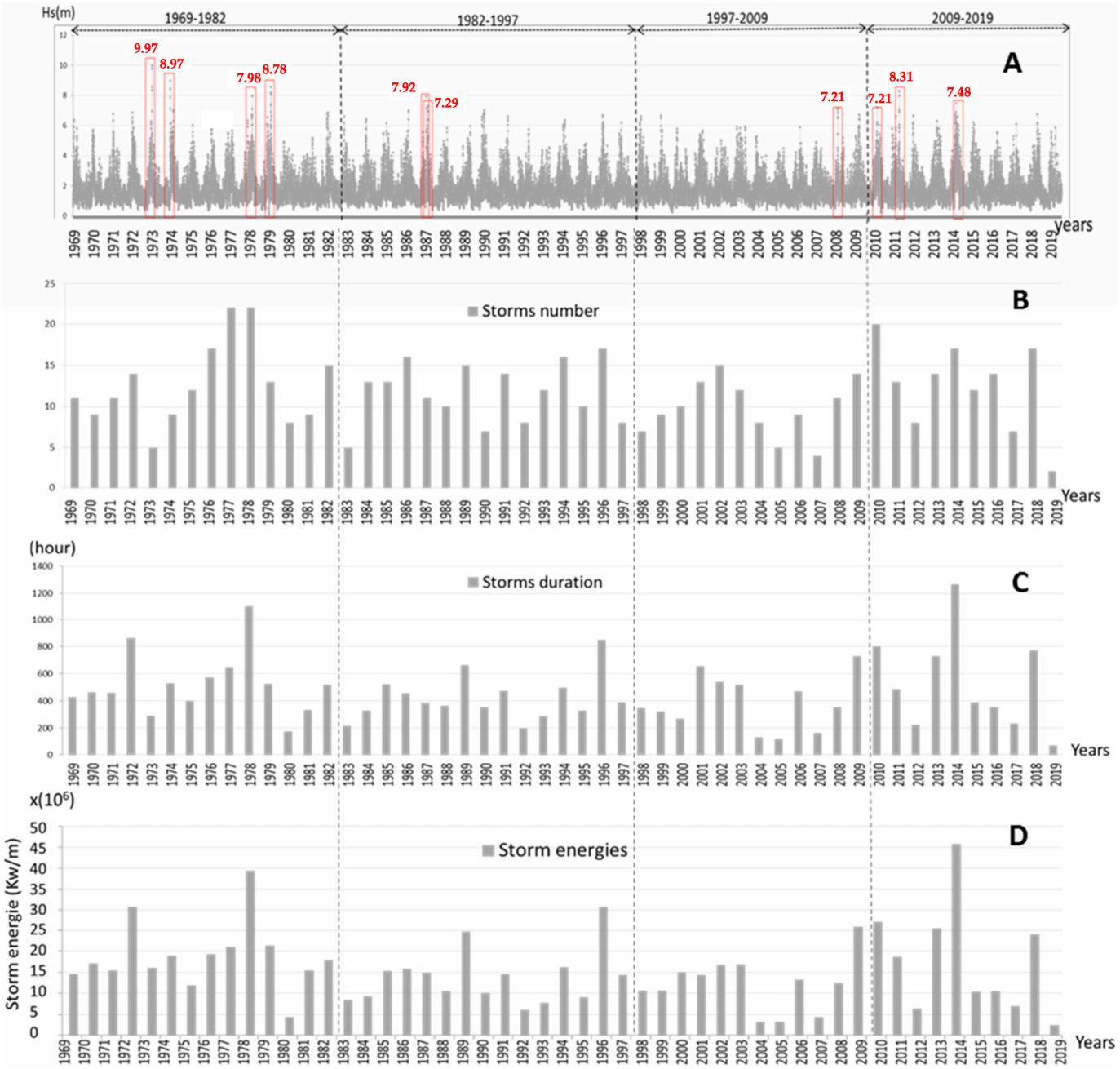

Figure 13. Yearly distribution of significant wave height (**A**), number of storms (**B**), storm duration (**C**), and storm energy (**D**) during the 1969–2020 period along the coastline of Casablanca–Mohammedia, modified from Chtioui et al. [46].

Coastal rates of change also help us implement shoreline monitoring services that aim to support the effective management of highly dynamic and constantly changing coastal environments with hazardous conditions, as well as for sustainable coastal zone management. In addition, rates of change from DE Africa can be combined with socio-economic risk factors for an integrated socio-environmental vulnerability assessment of coastal hazards [55]. Therefore, this study not only constitutes a significant contribution to coastal vulnerability assessment of Casablanca but also holds significant practical implications for scientists, managers, and policymakers to assess the impact of the range of drivers impacting the coastlines and potentially assist planning and forecasting for future scenarios for other regions and countries [35,36,56,57]. While our methodological framework builds on established CVI practices, the novelty lies in the operational use of DE Africa data combined

with topographic and lithological inputs to inform location-specific vulnerability assessments. The methodological simplicity supports reproducibility across other data-limited regions, while the spatial resolution and beach-level focus address key knowledge gaps in site-specific coastal risk evaluation. In addition, developing predictive shoreline models based on multi-temporal data represents a valuable direction for future studies, as it could provide critical insights into the expected trajectory of coastal change under various environmental and anthropogenic pressures. Such predictions would be essential for proactive planning, enabling coastal managers and policymakers to implement timely interventions, design resilient infrastructure, and minimize socio-economic and ecological impacts in vulnerable areas. Further research should explore how the spatial patterns of erosion and coastal vulnerability relate to regional oceanographic and meteorological drivers such as wave exposure, prevailing currents, and tidal range. Incorporating datasets such as ERA5 wave reanalysis, sediment budgets, or coastal modification records could provide valuable context for interpreting the physical processes underlying shoreline change. Therefore, information related to the state and the utilization of the coastline obtained from in situ documentations (Figure 14), combined with information obtained from remote-sensing datasets, is crucial for monitoring the coasts and managing coastal areas.

Figure 14. *Cont.*

Figure 14. Casablanca coastline landscape features obtained from field observations conducted on 6 August 2015. The coastline field documentation was performed by taking photographs of geologic

formation (**A**,**E**,**K**), instantaneous shoreline (**F**), urban extension (**B**,**D**,**F**,**J**), beach composition (**I**), and beach stabilizations (**L**) and utilization (**C**,**G**,**H**). Information obtained was later used for interpretation and the validation of remote-sensing results. These photographs were taken on the beach of the Anfa segment (**A**–**D**), on the neach of the La Corniche segment (**E**–**H**), and on the Beach of the Ain Diab segment (**I**–**L**).

5. Conclusions

The present study was undertaken to evaluate the coastal vulnerability of the Casablanca coastline due to climate change, using remote sensing and GIS. DE Africa Coastlines products and ASTER GDEM, combined with a geological map, allowed for the assessment of Casablanca's coastal vulnerability. Four variables were used to calculate the CVI: coastal geomorphology, coastal elevation, coastal slope, and coastal dynamics. The findings of this study can be summarized as follows:

1. Digital Earth Africa (DE Africa) coastlines products allowed us to conduct detailed analyses of shoreline dynamics from 2000 to 2023.
2. Around 44% to 23% of the studied areas have a very high to high vulnerability, particularly along sandy beach segments with low elevation. These areas are vulnerable to natural phenomena such as inundation, coastal flooding, and submersion.
3. Besides the Coastal Vulnerability Index assessment, DE Africa Coastlines products can further be used to develop coastal erosion indicators [58] and coastal erosion prediction models.

Supplementary Materials: The following are available online at https://www.mdpi.com/article/10.3390/rs17193370/s1. Detailed descriptions of point 0 considered for the showcase of the extraction of the coastal erosion metrics; the location of the 1630 points analyzed on the coast of Casablanca; the significance (p-value) values of the linear relationship between annual shoreline positions and the annual observations; the standard error of the linear relationship between annual shoreline positions and the annual observations; and charts depicting annual shoreline positions (cross-shore distances) for each point located on the Madame Choual, Ain Diab, Anfa, Ain Sebaa, Nahla, and Zenata Beaches, Casablanca, Morocco.

Author Contributions: Conceptualization, A.M.; methodology, A.M.; software, A.M.; validation, A.M.; formal analysis, A.M.; investigation, A.M.; resources, A.M.; data curation, A.M.; writing—original draft preparation, A.M.; writing—review and editing, C.T. and AM.; visualization, A.M.; supervision, A.M.; project administration, A.M.; funding acquisition, A.M. All authors have read and agreed to the published version of the manuscript.

Funding: This research received no external funding.

Conflicts of Interest: The authors declare no conflicts of interest.

Abbreviations

The following abbreviations are used in this manuscript:

ASTER GDEM (V2)	Advanced Spaceborne Thermal Emission and Reflection Radiometer Global Digital Elevation Model (version 2)
CVI	Coastal Vulnerability Index
DE Africa	Digital Earth Africa
DEM	Digital Elevation Model
EO	Earth Observation
EPR	End Point Rate
GIS	Geographic Information System
LRR	Linear Regression Rate
NSM	Net Shoreline Movement

PGA	Peak Ground Acceleration
PVI	Physical Vulnerability Index
SCE	Shoreline Change Envelope
SVI	Socio-Economic Vulnerability Index
WACA	West African Coastal Areas

Appendix A

Annual rates of change and coastline classification conducted on the Beach of Madame Choual.

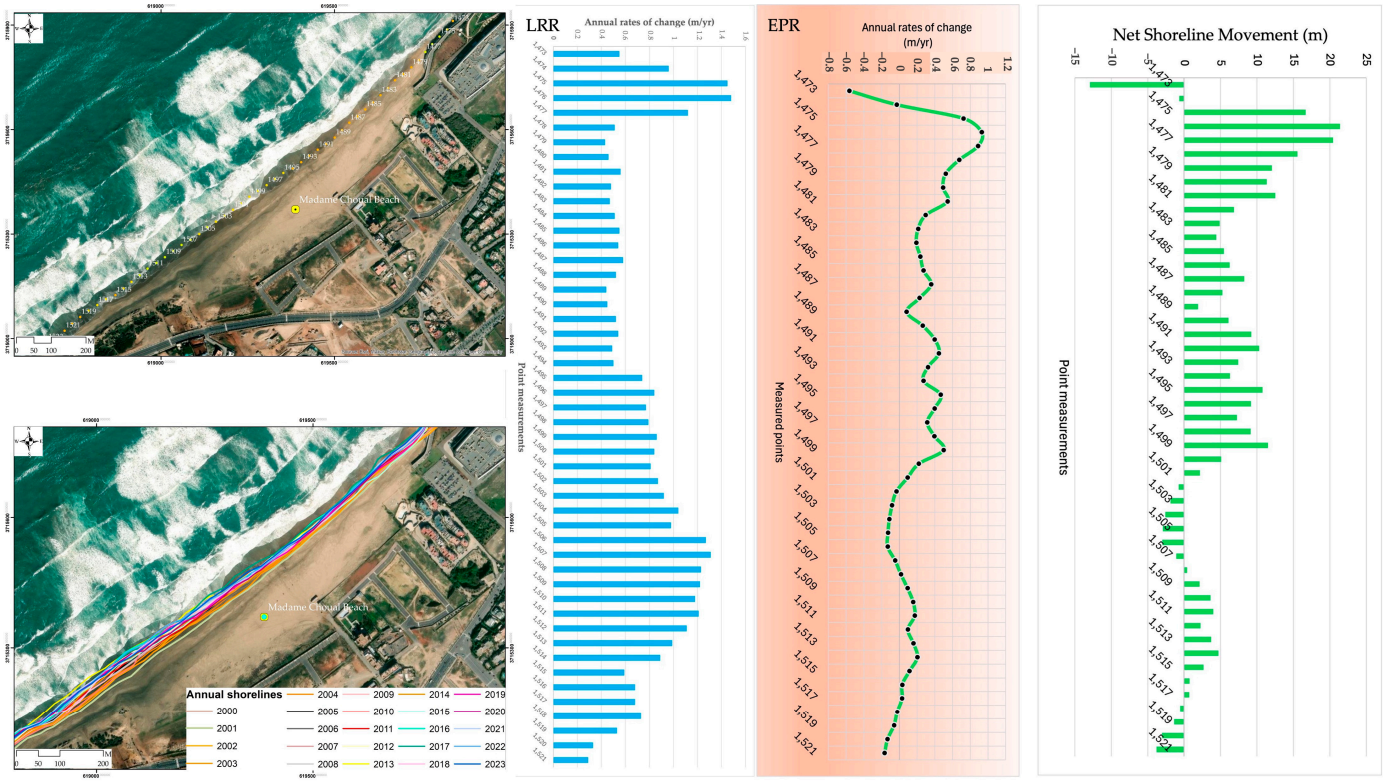

Figure A1. Annual shorelines and the location of 49 points containing annual rate-of-change values (LRR and EPR) and Net Shoreline Movement (NSM) for the Beach of Madame Choual. The points are labeled from the NE (point 1473) to the SW (point 1521), with an interval of 30 m. For each point, annual rates of change were calculated from 2000 to 2023. LRR revealed the coastline growth of about 1.5 m/yr, while EPR indicated the coastline growth of about 0.9 m/yr and a retreat of about −0.6 m/yr. The NSM indicates that the direction of longshore transport is SW to NE. Details on cross-shore annual shoreline positions are presented in Supplementary Materials S.5 (Figures S4–S6 and S8).

Table A1. Annual rates of change and coastline classification results obtained for the Beach of Madame Choual.

Rate of Change Range (m/yr)	LRR (%)	EPR (%)	Coastline Classification	CVI Ranking
<−2	N. A	N. A	Very high erosion	Very high
<−1–≥−2	N. A	N. A	High erosion	High
<0–≥−1	N. A	24.45	Moderate erosion	Moderate
>0–≤+1	77.55	75.55	Accretion	Low
>+1	22.45	N. A	Moderate accretion	

Annual rates of change and coastline classification conducted on Ain Diab beach.

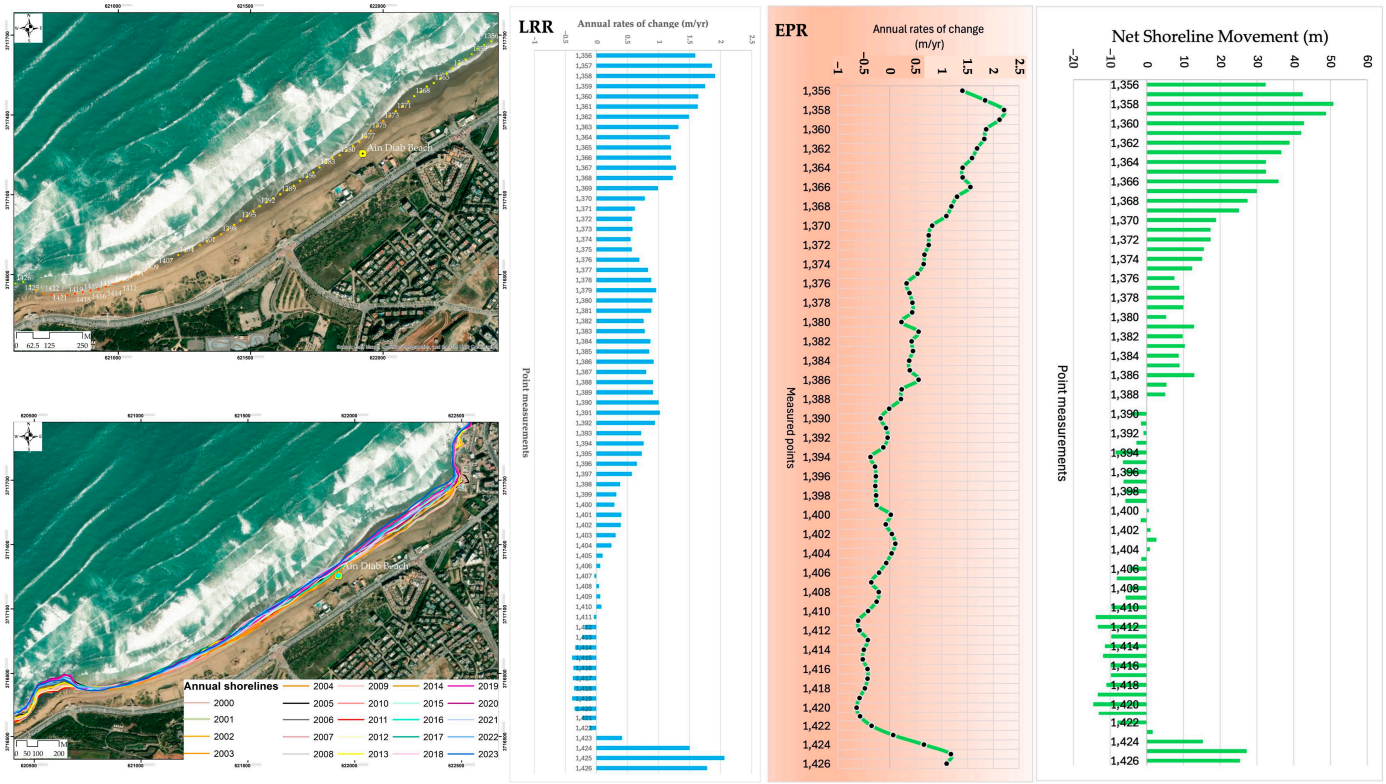

Figure A2. Annual shorelines and the location of 71 points containing annual rate-of-change values (LRR and EPR) and Net Shoreline Movement (NSM) for the Beach of Ain Diab. The points are labeled from the NE (point 1356) to the SW (point 1426), with an interval of 30 m. For each point, annual rates of change were calculated from 2000 to 2023. LRR revealed the coastline growth of about 2 m/yr and retreat of about −0.4 m/yr, while EPR indicated the coastline growth of about 2.3 m/yr and a retreat of about −0.55 m/yr. The NSM indicates that the direction of longshore transport is SW to NE. Details on cross-shore annual shoreline positions are presented in Supplementary Materials S.6 (Figures S8–S12).

Table A2. Annual rates of change and coastline classification results obtained for the Beach of Ain Diab.

Rate of Change Range (m/yr)	LRR (%)	EPR (%)	Coastline Classification	CVI Ranking
<−2	N. A	N. A	Very high erosion	Very high
<−1–≥−2	N. A	N. A	High erosion	High
<0–≥−1	18.30	42.25	Moderate erosion	Moderate
>0–≤+1	56.34	35.21	Accretion	Low
>+1	25.36	22.54	Moderate accretion	

Annual rates of change and coastline classification conducted on the Beach of Anfa.

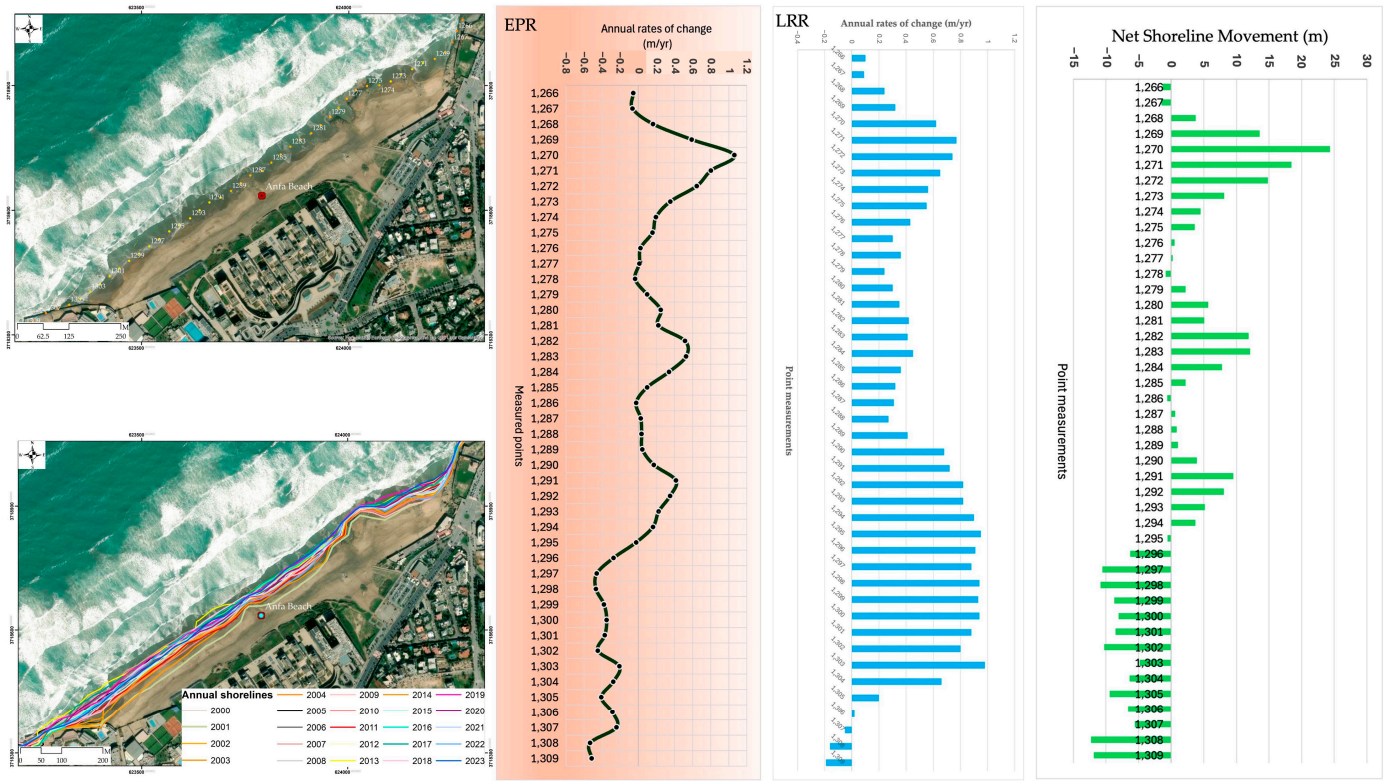

Figure A3. Annual shorelines and the location of 44 points containing annual rate-of-change values (LRR and EPR) and Net Shoreline Movement (NSM) for the Beach of Anfa. The points are labeled from the NE (point 1266) to the SW (point 1309), with an interval of 30 m. For each point, annual rates of change were calculated from 2000 to 2023. LRR revealed the coastline growth of about 1 m/yr and retreat of about −0.2 m/yr, while EPR indicated the coastline growth of about 1.09 m/yr and a retreat of about −0.5 m/yr. The NSM indicates that the direction of longshore transport is SW to NE. Details on cross-shore annual shoreline positions are presented in Supplementary Materials S.7 (Figures S13–S15).

Table A3. Annual rates of change and coastline classification results obtained for the Beach of Anfa.

Rate of Change Range (m/yr)	LRR (%)	EPR (%)	Coastline Classification	CVI Ranking
<−2	N. A	N. A	Very high erosion	Very high
<−1–≥−2	N. A	N. A	High erosion	High
<0–≥−1	6.82	38.63	Moderate erosion	Moderate
>0–≤+1	93.18	59.1	Accretion	Low
>+1	N. A	2.27	Moderate accretion	

Annual rates of change and coastline classification conducted on Ain Sebaa Beach.

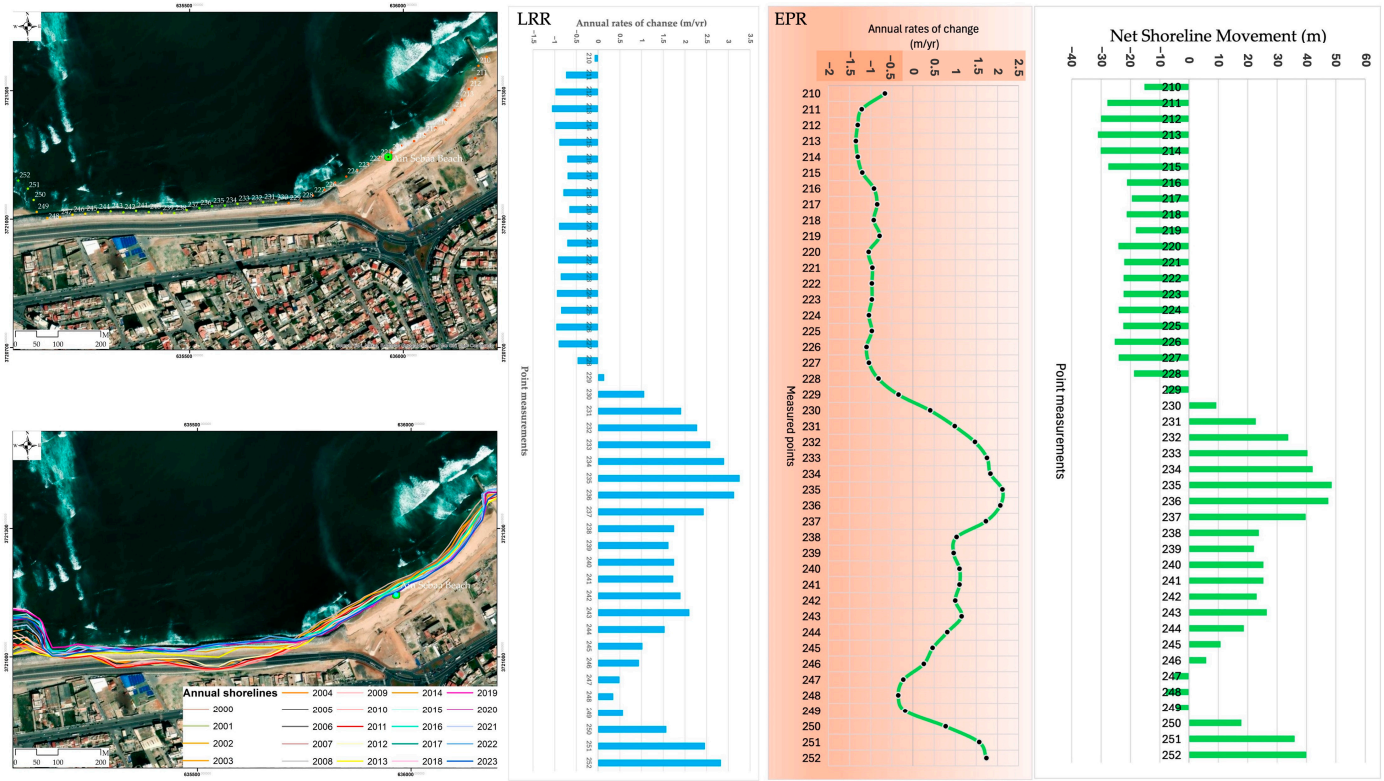

Figure A4. Annual shorelines and the location of 43 points containing annual rate-of-change values (LRR and EPR) and Net Shoreline Movement (NSM) for the Beach of Ain Sebaa. The points are labeled from the NE (point 210) to the SW (point 252), with an interval of 30 m. For each point, annual rates of change were calculated from 2000 to 2023. LRR revealed the coastline growth of about 3.4 m/yr and retreat of about −1 m/yr, while EPR indicated the coastline growth of about 2.09 m/yr and a retreat of about −1.45 m/yr. The NSM indicates that the direction of longshore transport is NE to SW. Details on cross-shore annual shoreline positions are presented in Supplementary Materials S.8 (Figures S16–S18).

Table A4. Annual rates of change and coastline classification results obtained for the Beach of Ain Sebaa.

Rate of Change Range (m/yr)	LRR (%)	EPR (%)	Coastline Classification	CVI Ranking
<−2	N. A	N. A	Very high erosion	Very high
<−1–≥−2	4.66	16.28	High erosion	High
<0–≥−1	37.2	39.53	Moderate erosion	Moderate
>0–≤+1	11.63	20.93	Accretion	Low
>+1	46.51	23.26	Moderate accretion	

Annual rates of change and coastline classification conducted on the Beach of Nahla.

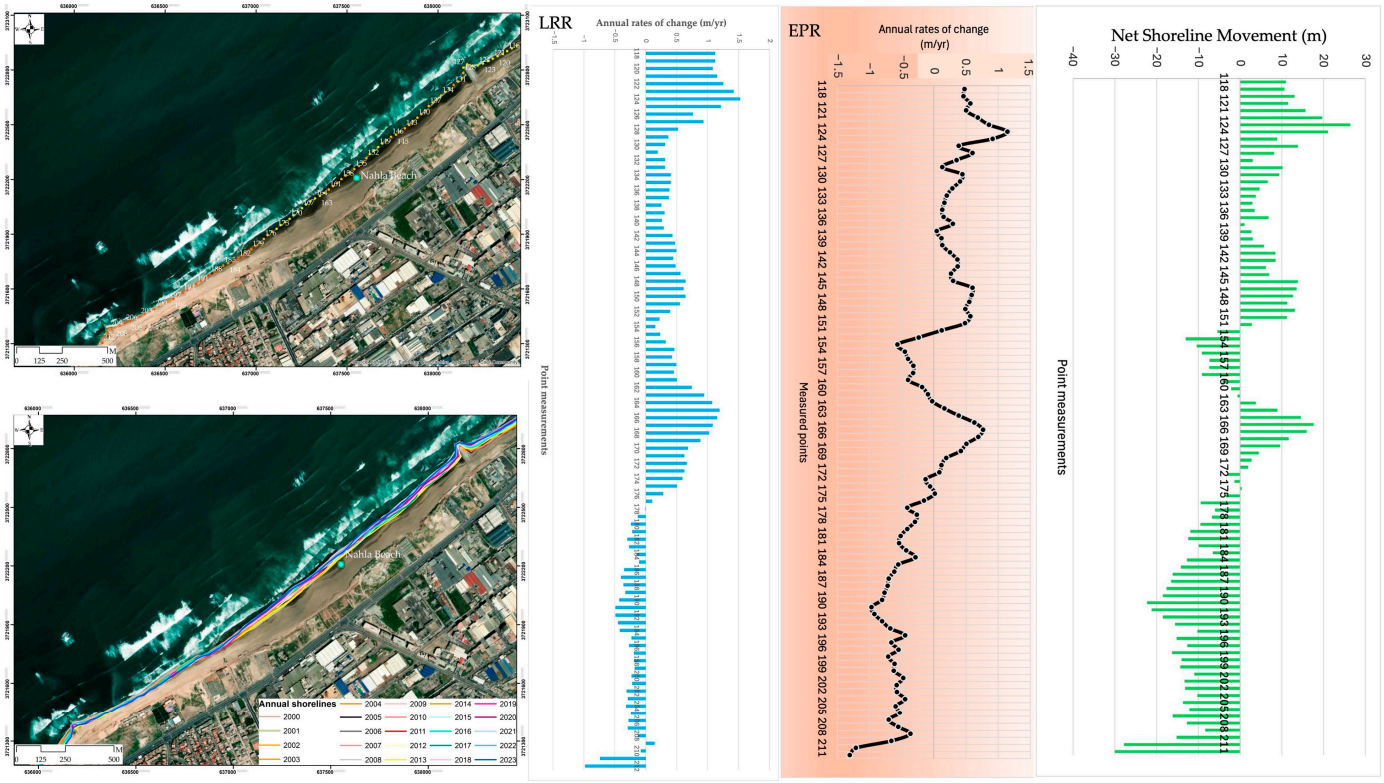

Figure A5. Annual shorelines and the location of 95 points containing annual rate-of-change values (LRR and EPR) and Net Shoreline Movement (NSM) for the Beach of Nahla. The points are labeled from the NE (point 118) to the SW (point 212), with an interval of 30 m. For each point, annual rates of change were calculated from 2000 to 2023. LRR revealed the coastline growth of about 1.5 m/yr and retreat of about −1 m/yr, while EPR indicated the coastline growth of about 1.2 m/yr and a retreat of about −1.3 m/yr. The NSM indicates that the direction of longshore transport is SW to NE. Details on cross-shore annual shoreline positions are presented in Supplementary Materials S.9 (Figures S19–S25).

Table A5. Annual rates of change and coastline classification results obtained for the Beach of Nahla.

Rate of Change Range (m/yr)	LRR (%)	EPR (%)	Coastline Classification	CVI Ranking
<−2	N. A	N. A	Very high erosion	Very high
<−1–≥−2	N. A	2.11	High erosion	High
<0–≥−1	37.90	48.42	Moderate erosion	Moderate
>0–≤+1	48.42	48.42	Accretion	Low
>+1	13.68	1.05	Moderate accretion	

Annual rates of change and coastline classification conducted on the Beach of Zenata.

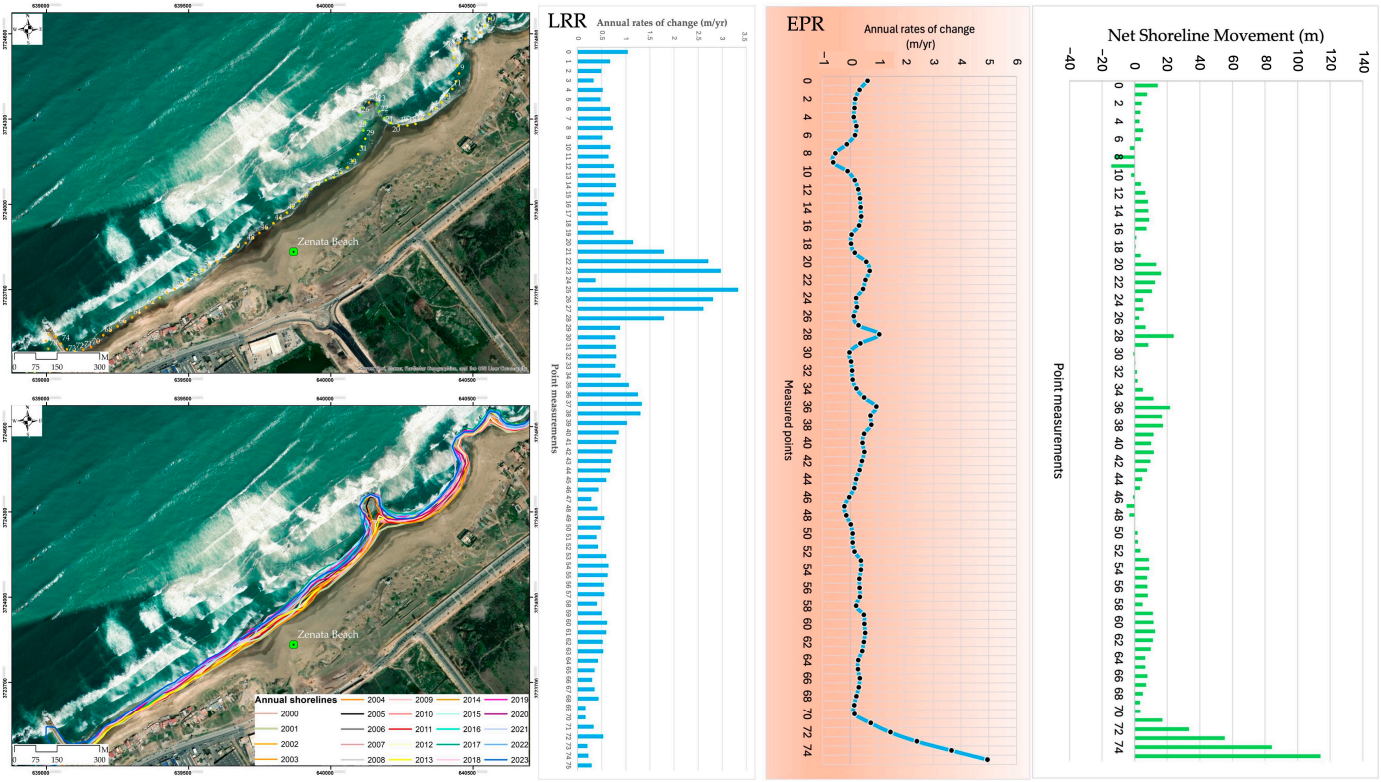

Figure A6. Annual shorelines and the location of 76 points containing annual rate-of-change values (LRR and EPR) and Net Shoreline Movement (NSM) for the Beach of Zenata. The points are labeled from the NE (point 0) to the SW (point 75), with an interval of 30 m. For each point, annual rates of change were calculated from 2000 to 2023. LRR revealed the coastline growth of about 3.4 m/yr while EPR indicated the coastline growth of about 5 m/yr and a retreat of about −0.6 m/yr. The NSM indicates that the direction of longshore transport is NE to SW. Details on cross-shore annual shoreline positions are presented in Supplementary Materials S.10 (Figures S26–S30).

Table A6. Annual rates of change and coastline classification results obtained for the Beach of Zenata.

Rate of Change Range (m/yr)	LRR (%)	EPR (%)	Coastline Classification	CVI Ranking
<−2	N. A	N. A	Very high erosion	Very high
<−1–≥−2	N. A	N. A	High erosion	High
<0–≥−1	N. A	10.53	Moderate erosion	Moderate
>0–≤+1	17.11	81.58	Accretion	Low
>+1	8289	7.89	Moderate accretion	

References

1. Noor, N.M.; Abdul Maulud, K.N. Coastal Vulnerability: A Brief Review on Integrated Assessment in Southeast Asia. *J. Mar. Sci. Eng.* **2022**, *10*, 595. [CrossRef]
2. Toumasi, P.; Petropoulos, G.P.; Detsikas, S.E.; Kalogeropoulos, K.; Tselos, N.G. Coastal Vulnerability Impact Assessment under Climate Change in the Arctic Coasts of Tromsø, Norway. *Earth* **2024**, *5*, 640–653. [CrossRef]
3. Ortiz, P.; López, I.; Pagán, J.I. Assessment of Beach Erosion Vulnerability in the Province of Valencia, Spain. *J. Mar. Sci. Eng.* **2024**, *12*, 2111. [CrossRef]
4. Tadić, A.; Krvavica, N.; Benac, Č.; Ružić, I. Coastal vulnerability index for the indented coastline of Primorje-Gorski Kotar County, Croatia. *Reg. Stud. Mar. Sci.* **2024**, *80*, 103862. [CrossRef]
5. Rocha, C.; Antunes, C.; Catita, C. Coastal Indices to Assess Sea-Level Rise Impacts—A Brief Review of the Last Decade. *Ocean. Coast. Manag.* **2023**, *237*, 106536. [CrossRef]

6. Handiani, D.N.; Heriati, A.; Gunawan, W.A. Comparison of Coastal Vulnerability Assessment for Subang Regency in North Coast West Java-Indonesia. *Geomat. Nat. Hazards Risk* **2022**, *13*, 1178–1206. [CrossRef]
7. Koroglu, A.; Ranasinghe, R.; Jiménez, J.A.; Dastgheib, A. Comparison of coastal vulnerability index applications for Barcelona Province. *Ocean Coast. Manag.* **2019**, *178*, 104799. [CrossRef]
8. Theocharidis, C.; Prodromou, M.; Doukanari, M.; Kalogirou, E.; Eliades, M.; Kontoes, C.; Hadjimitsis, D.; Neocleous, K. Integrated Coastal Vulnerability Index (ICVI) Assessment of Protaras Coast in Cyprus: Balancing Tourism and Coastal Risks. *Geographies* **2025**, *5*, 12. [CrossRef]
9. Gornitz, V. Vulnerability of the East Coast, USA to future sea level rise. *J. Coast. Res.* **1990**, *9*, 201–237.
10. Thieler, E.R.; Hammar-Klose, E.S. *National Assessment of Coastal Vulnerability to Sea-Level Rise: Preliminary Results for the U.S. Atlantic Coast*; United States Geological Survey: Reston, VA, USA, 1999.
11. Pendleton, E.A.; Thieler, E.R.; Williams, S.J.; Beavers, R.L. *Coastal Vulnerability Assessment of Padre Island National Seashore (PAIS) to Sea-Level Rise*; US Geological Survey: Reston, VA, USA, 2004.
12. Alcántara-Carrió, J.; Echavarría, L.M.G.; Jaramillo-Vélez, A. Is the coastal vulnerability index a suitable index? Review and proposal of alternative indices for coastal vulnerability to sea level rise. *Geo-Mar. Lett.* **2024**, *44*, 8. [CrossRef]
13. Šimac, Z.; Lončar, N.; Faivre, S. Overview of Coastal Vulnerability Indices with Reference to Physical Characteristics of the Croatian Coast of Istria. *Hydrology* **2023**, *10*, 14. [CrossRef]
14. Angulo, R.J.; Lessa, G.C.; Souza, M.C. A critical review of Mid- to Late-Holocene sea-level fluctuations on the eastern Brazilian coastline. *Quat. Sci. Rev.* **2006**, *25*, 486–506. [CrossRef]
15. Sun, W.; Chen, C.; Weiwei, L.; Yang, G.; Meng, X.; Wang, L.; Ren, K. Coastline extraction using remote sensing: A review. *GISci. Remote Sens.* **2023**, *60*, 2243671. [CrossRef]
16. Zhou, X.; Wang, J.; Zheng, F.; Wang, H.; Yang, H. An Overview of Coastline Extraction from Remote Sensing Data. *Remote Sens.* **2023**, *15*, 4865. [CrossRef]
17. Pantusa, D.; D'Alessandro, F.; Frega, F.; Francone, A.; Tomasicchio, G.R. Improvement of a Coastal Vulnerability Index and Its Application along the Calabria Coastline, Italy. *Sci. Rep.* **2022**, *12*, 21959. [CrossRef] [PubMed]
18. Manno, G.; Azzara, G.; Re, C.L.; Martinello, C.; Basile, M.; Rotigliano, E.; Ciraolo, G. An Approach for the Validation of a Coastal Erosion Vulnerability Index: An Application in Sicily. *J. Mar. Sci. Eng.* **2022**, *11*, 23. [CrossRef]
19. Borzì, L.; Anfuso, G.; Manno, G.; Distefano, S.; Urso, S.; Chiarella, D.; Di Stefano, A. Shoreline Evolution and Environmental Changes at the NW Area of the Gulf of Gela (Sicily, Italy). *Land* **2021**, *10*, 1034. [CrossRef]
20. Foti, G.; Barbaro, G.; Barillà, G.C.; Mancuso, P.; Puntorieri, P. Shoreline Evolutionary Trends Along Calabrian Coasts: Causes and Classification. *Front. Mar. Sci.* **2022**, *9*, 846914. [CrossRef]
21. Castelle, B.; Masselink, G.; Scott, T.; Stokes, C.; Konstantinou, A.; Marieu, V.; Bujan, S. Satellite-derived shoreline detection at a high-energy meso-macrotidal beach. *Geomorphology* **2021**, *383*, 107707. [CrossRef]
22. Konstantinou, A.; Scott, T.; Masselink, G.; Stokes, K.; Conley, D.; Castelle, B. Satellite-based shoreline detection along high-energy macrotidal coasts and influence of beach state. *Mar. Geol.* **2023**, *462*, 107082. [CrossRef]
23. Luijendijk, A.P.; Kras, E.; Dagalaki, V.; Morelissen, R.; Hoteit, I.; Ranasinghe, R. Regime Shifts in Future Shoreline Dynamics of Saudi Arabia. *Front. Mar. Sci.* **2022**, *8*, 798657. [CrossRef]
24. Darwish, K.; Smith, S. Landsat-Based Assessment of Morphological Changes along the Sinai Mediterranean Coast between 1990 and 2020. *Remote Sens.* **2023**, *15*, 1392. [CrossRef]
25. Bishop-Taylor, R.; Nanson, R.; Sagar, S.; Lymburner, L. Mapping Australia's Dynamic Coastline at Mean Sea Level Using Three Decades of Landsat Imagery. *Remote Sens. Environ.* **2021**, *267*, 112734. [CrossRef]
26. Nanson, R.; Bishop-Taylor, R.; Sagar, S.; Lymburner, L. Geomorphic insights into Australia's coastal change using a national dataset derived from the multi-decadal Landsat archive. *Estuar. Coast. Shelf Sci.* **2022**, *265*, 107712. [CrossRef]
27. Digital Earth Africa. Available online: https://www.digitalearthafrica.org/ (accessed on 22 April 2025).
28. DE Africa Coastline Data availability. Digital Earth Africa Coastlines. Available online: https://registry.opendata.aws/deafrica-coastlines (accessed on 22 April 2025).
29. Naji, E.M.; Aberkan, M.; Saadane, A.; Nmiss, M. Erosion and shoreline retreat indicators in the Rabat-Salé littoral and their impact on coastal planning. *J. Afr. Earth Sci.* **2025**, *223*, 105534. [CrossRef]
30. Moussaid, J.; Fora, A.A.; Zourarah, B.; Maanan, M.; Maanan, M. Using automatic computation to analyse the rate of shoreline change on the Kenitra coast, Morocco. *Ocean Eng.* **2015**, *102*, 71–77. [CrossRef]
31. Aangri, A.; Hakkou, M.; Krien, Y.; Benmohammadi, A. Predicting Shoreline Change for the Agadir and Taghazout Coasts (Morocco). *J. Coast. Res.* **2022**, *38*, 937–950. [CrossRef]
32. Benkhattab, F.Z.; Hakkou, M.; Bagdanavičiūtė, I.; Mrini, A.E.; Zagaoui, H.; Rhinane, H.; Maanan, M. Spatial–temporal analysis of the shoreline change rate using automatic computation and geospatial tools along the Tetouan coast in Morocco. *Nat. Hazards* **2020**, *104*, 519–536. [CrossRef]

33. Heger, M.; Vashold, L.M.; Carpenter, S.; Toquica, O.M.A. *Coastal Erosion and Its Costs in the Maghreb: Disappearing Coasts*; World Bank: Washington, DC, USA, 2023; report no. 179616.
34. Oussama, L. Approche Multidisciplinaire de Suivi de la Dynamique Marine du Littoral de Mohammedia. Master's Thesis, Université Cadi Ayyad, Marrakesh, Morocco, 2013; pp. 24–25.
35. Coastlines Monitoring Data Description. Available online: https://docs.digitalearthafrica.org/en/latest/data_specs/Coastlines_specs.html (accessed on 22 April 2025).
36. DE Africa Use Case. Monitoring Coastal Erosion Along Africa's Coastline. Available online: https://docs.digitalearthafrica.org/en/latest/sandbox/notebooks/Real_world_examples/Coastal_erosion.html (accessed on 22 April 2025).
37. Zhang, K.; Gann, D.; Ross, M.; Robertson, Q.; Sarmiento, J.; Santana, S.; Rhome, J.; Fritz, C. Accuracy assessment of ASTER, SRTM, ALOS and TDX DEMs for Hispaniola and implications for mapping vulnerability to coastal flooding. *Remote Sens. Environ.* **2019**, *225*, 290–306. [CrossRef]
38. Tachikawa, T.; Kaku, M.; Iwasaki, A.; Gesch, D.B.; Oimoen, M.J.; Zhang, Z.; Danielson, J.J.; Krieger, T.; Curtis, B.; Haase, J. *ASTER Global Digital Elevation Model Version 2—Summary of Validation Results*; NASA: Washington, DC, USA, 2011.
39. Mahesh, R.; Sarunjith, K.J.; Rajakumari, S.; Muruganandam, R.; Ramesh, R. Quality assessment of open sourced digital elevation models in southeast coast of India. *Egypt. J. Remote Sens. Space Sci.* **2021**, *24*, 745–754.
40. Zerhouny, M.; Fadil, A.; Hakdaoui, M. Underground Space Utilization in the Urban Land-Use Planning of Casablanca (Morocco). *Land* **2018**, *7*, 143. [CrossRef]
41. Omira, R.; Baptista, M.A.; Matias, L.; Miranda, J.M.; Catita, C.; Carrilho, F.; Toto, E. Design of a Sea-level Tsunami Detection Network for the Gulf of Cadiz. *Nat. Hazards Earth Syst. Sci.* **2009**, *9*, 1327–1338. [CrossRef]
42. Egis bceom international/iau-idf/brgm. *Adaptation au Changement Climatique et aux Désastres Naturels des villes Côtières D'afrique du Nord, Phase 1: Évaluation des Risques en Situation Actuelle et à L'horizon 2030 pour la ville de Casablanca Version finale*; World Bank: Washington, DC, USA, 2011; pp. 17–25, 33–52, 70–80.
43. Stoa, R. The Coastline Paradox. *Rutgers Univ. Law Rev.* **2020**, *72*, 50. [CrossRef]
44. Horn, B.K. Hill Shading and the Reflectance Map. *Proc. IEEE* **1981**, *69*, 14–47. [CrossRef]
45. Pepe, G.; Coutu, G. Beach morphology change study using ArcGIS spatial analyst. *Middle States Geogr.* **2008**, *41*, 91–97.
46. Chtioui, T.; Hakkou, M.; Abdelhaq, A.; Benmohammadi, A.; Maanane, M. Storm's influence on long-term shoreline evolution along Casablanca-Mohammedia (Morocco). *Reg. Stud. Mar. Sci.* **2024**, *75*, 103549.
47. Chtioui, T.; Hakkou, M.; Aangri, A.; El Hassani, F.; El Mostafa, Z.; Benmohammadi, A. Assessing coastal flood risk under extreme events and sea level rise in the Casablanca-Mohammedia coastline (Morocco). *Nat. Hazards* **2024**, *120*, 10727–10752. [CrossRef]
48. Muzirafuti, A. Africa's Coastline Long-Term Monitoring Using Remote Sensing and GIS Techniques. In Proceedings of the 2025 International Workshop on Metrology for the Sea, Learning to Measure Sea Health Parameters (MetroSea), Genova, Italy, 8–10 October 2025.
49. Jonah, F.E.; Boateng, I.; Osman, A.; Shimba, M.J.; Mensah, E.A.; Adu-Boahen, K.; Chuku, E.O.; Effah, E. Shoreline change analysis using end point rate and net shoreline movement statistics: An application to Elmina, Cape Coast and Moree section of Ghana's coast. *Reg. Stud. Mar. Sci.* **2016**, *7*, 19–31. [CrossRef]
50. Aladwani, N.S. Shoreline Change Rate Dynamics Analysis and Prediction of Future Positions Using Satellite Imagery for the Southern Coast of Kuwait: A Case Study. *Oceanologia* **2022**, *64*, 417–432. [CrossRef]
51. de Lima, L.T.; Fernández-Fernández, S.; de Almeida Espinoza, J.M.; da Guia Albuquerque, M.; Bernardes, C. End Point Rate Tool for QGIS (EPR4Q): Validation Using DSAS and AMBUR. *ISPRS Int. J. Geo-Inf.* **2021**, *10*, 162. [CrossRef]
52. Laksono, F.A.T.; Borzì, L.; Distefano, S.; Di Stefano, A.; Kovács, J. Shoreline Prediction Modelling as a Base Tool for Coastal Management: The Catania Plain Case Study (Italy). *J. Mar. Sci. Eng.* **2022**, *10*, 1988. [CrossRef]
53. Muzirafuti, A.; Lanza, S.; Paltrinieri, D.; Faina, G.; El Hafyani, M.; Randazzo, G. Geomorphology in the Digital Age: A Case Study Project of Quantitative Geomorphology from Images. In Proceedings of the 2023 International Workshop on Metrology for the Sea; Learning to Measure Sea Health Parameters (MetroSea), La Valletta, Malta, 4–6 October 2023; pp. 513–518.
54. Cao, T.; Han, D.; Song, X. Past, present, and future of global seawater intrusion research: A bibliometric analysis. *J. Hydrol.* **2021**, *603*, 126844. [CrossRef]
55. Tanim, A.H.; Goharian, E.; Moradkhani, H. Integrated socio-environmental vulnerability assessment of coastal hazards using data-driven and multi-criteria analysis approaches. *Sci. Rep.* **2022**, *12*, 11625. [CrossRef] [PubMed]
56. Muzirafuti, A.; Cascio, M.; Lanza, S.; Randazzo, G. UAV Photogrammetry-based Mapping of the Pocket Beaches of Isola Bella Bay, Taormina (Eastern Sicily). In Proceedings of the 2021 International Workshop on Metrology for the Sea, Learning to Measure Sea Health Parameters (MetroSea), Reggio Calabria, Italy, 4–6 October 2021; pp. 418–422.

57. Muzirafuti, A.; Crupi, A.; Lanza, S.; Barreca, G.; Randazzo, G. Shallow water bathymetry by satellite image: A case study on the coast of San Vito Lo Capo Peninsula, Northwestern Sicily, Italy. In Proceedings of the 2019 IMEKO TC19 International Workshop on Metrology for the Sea: Learning to Measure Sea Health Parameters, MetroSea 2019, Genoa, Italy, 3–5 October 2019; pp. 129–134.
58. McCarroll, R.J.; David, M.K.; Jin, L.; Allan, B.; Ierodiaconou, D. Design and application of coastal erosion indicators using satellite and drone data for a regional monitoring program. *Ocean Coast. Manag.* **2024**, *253*, 107146. [CrossRef]

Disclaimer/Publisher's Note: The statements, opinions and data contained in all publications are solely those of the individual author(s) and contributor(s) and not of MDPI and/or the editor(s). MDPI and/or the editor(s) disclaim responsibility for any injury to people or property resulting from any ideas, methods, instructions or products referred to in the content.